

ISBN: 978-605-69034-6-5



**NURE**

Kharkiv National University of Radio  
Electronics



AZERBAIJAN UNIVERSITY



**ESKİŞEHİR TEKNİK ÜNİVERSİTESİ**  
ESKİŞEHİR TECHNICAL UNIVERSITY

# ICONAT 2020

**BAKU-AZERBAIJAN**  
**AUGUST 20-22, 2020**

**INTERNATIONAL CONFERENCE**

**ON**

**NATURAL SCIENCE AND TECHNOLOGY**

## ABSTRACT BOOK

[www.iconat-2020.com](http://www.iconat-2020.com)

## **CHAIRMAN OF CONFERENCE**

Prof. Dr. Saadat Namig Aliyeva-Rector (Honor of Conference), Azerbaijan University, Azerbaijan.

## **ORGANIZING COMMITTEE**

Prof. Dr. Omarov Murad, Vice-Rector, NURE, (Ukraine)

Prof. Dr. Gürsoy Arslan, Vice-Rector, Eskisehir Technical University, Turkey.

Prof. Dr. Yusif Gasimov, Vice-Rector, Azerbaijan University, Azerbaijan.

Prof. Dr. Zafer Demir, Eskisehir Technical University, Turkey.

Prof. Dr. Abidin Kılıç (Chairman of Organization Committee), Eskisehir Technical University, Turkey

Prof. Dr. Asif Pashayev, Azerbaijan University, Azerbaijan.

## **International Scientific Committee**

Prof. Dr. Andrii Chukhrai (Ukraine)

Prof. Dr. Oleg Lazarenko (Ukraine)

Prof. Dr. Dmytro Fedasyuk (Ukraine)

Prof. Dr. Dursun Aydın (Turkey)

Prof. Dr. Oleksandr Lemeshko (Ukraine)

Prof. Dr. Kadir Aslan (USA)

Prof. Dr. Marzena S. Mlichalowska (Poland)

Assoc. Prof. Dr. Haluk Yapıcıoğlu (Turkey)

Prof. Dr. Khanmammadov Agil (Azerbaijan)

Prof. Farajov Araz (Azerbaijan)

Prof. Dr. Tayfun Akin (Turkey)

Prof. Dr. Ekrem Aydın (Turkey)

Prof. Dr. Volodymyr Storozhenko (Ukraine)

Prof. Dr. Yevgen Nelin (Ukraine)

Senior Lecturer Mirzabayli Gunduz (Azerbaijan)

Prof. Dr. Khanmammadov Agil (Azerbaijan)

Prof. Dr. Hüseyin Sarı (Turkey)

Prof. Dr. Igor Ruzhentsev (Ukraine)

Prof. Dr. Hüseyin Sarı (Turkey)

Igor Nevlidov (Ukraine)

Azizov Bahram (Azerbaijan)

Prof. Dr. Sevil Çetinkaya Gürer (Turkey)

Prof. Dr. Süleyman Demir (Turkey)

Lecturer Gafarova Nigar (Azerbaijan)

Sen. Lecturer Akhmadov Abilhasan (Azerbaijan)

Assoc. Professor Abbasov Teymur (Azerbaijan)

Assoc. Prof. Arzu Guliyev (Azerbaijan)

Prof. Dr. Arturas Mickus (Lithuania)

Prof. Dr. Cengiz Türe (Turkey)

Prof. Dr. Oleh Avrunin (Ukraine)

Prof. Dr. İsmail Sökmen (Turkey)

Prof. Dr. Ekrem Gürel (Turkey)

Prof. Dr. Feridun Ay (Turkey)

Prof. Dr. Huseynov Hidayet (Azerbaijan)

Prof. Dr. Mehmet Candan (Turkey)

Prof. Dr. Saliha Ilıcan (Turkey)

Prof. Dr. Yüksel Ergün (Turkey)

Prof. Dr. Oguz Gülseren (Turkey)

Prof. Dr. Yuri Machekhin (Ukraine)

Prof. Dr. Yevgenii Bodyansky (Ukraine)

Prof. Dr. Valentin Filatov (Ukraine)

Prof. Dr. Valentin Filatov (Ukraine)

Prof. Dr. Oleksandr Tsopa (Ukraine)

Prof. Dr. Rauf Amirov (Turkey)

Prof. Dr. Mustafa Hoştut (Turkey)

Assoc. Professor Shirinov Rasim (Azerbaijan) Prof. Dr.

Assoc. Prof. Dr. Nihal Kus (Turkey) Assoc. Professor

Dr. Aliyev Gabil (Azerbaijan)

Dr. Latifa Aghamalieva (Azerbaijan)

Senior Lecturer Aghayeva Nurdan (Azerbaijan) Senior

Prof. Dr. Svetlana Kashuba (Poland)

Prof. Dr. Murat Tanışlı (Turkey)

Prof. Dr. Urfat Nuriyev (Turkey)

**Official Opening of the ICONAT-2020**

**20 August 2020      Meeting Salon I – Azerbaijan University**

09.00      The Start of Registration Process

10.30      Official Opening of the ICONAT-2020  
Welcome by Conference

**Meeting ID: 964 5238 2438**

**Passcode: 382819**

Prof. Dr. Saadat Namig Aliyeva-Rector, Azerbaijan University, Azerbaijan

Prof. Dr. Gürsoy Arslan, Vice-Rector, Eskisehir Technical University, Turkey

Prof. Dr. Omarov Murad, Vice-Chairman (ICONAT 2020)  
Vice-Rector, NURE, (Ukraine)

Prof. Dr. Abidin Kılıç, Eskisehir Technical University, Turkey  
Member of ICONAT 2020 Organization Committee

11.00      Invited Speaker  
Prof. Dr. Yüksel Ergun (Turkey)  
Terahertz QWIP Using Asymmetric Quantum Wells

12.00      **Lunch Break**

**20.08.2020 Thursday**

| ORAL PRESENTATIONS |   |   |
|--------------------|---|---|
|                    | <b>Chairing</b><br><b>Assoc. Prof. Dr. Sedef Dikmen</b> | <b>Hall 1</b> <b>Meeting ID: 986 0786 6678</b><br><b>14.00</b> <b>Passcode: 221183</b>                          |
| 01                 | Kevser Köklü<br>Turkey                                  | Solution Of Logarithmic Kernel Integral Equations By Natural Transform  |
| 02                 | Guram Chaganava<br>Georgia                              | Keypoint Detector Retraining Techniques For The Communication System Of Sign Language Speakers                  |
| 03                 | Nihal Kuş<br>Turkey                                     | Theoretical and Experimental Vibrational Spectrum Analysis of Ionic Liquid 1-Ethyl-3-Methylimidazolium Chloride |
|                    |   |   |

| ORAL PRESENTATIONS |   |  |
|--------------------|---|--|
|                    | <b>Chairing</b><br><b>Assist. Prof. Dr. Utku Kaya</b> | <b>Hall 2</b> <b>Meeting ID: 932 8681 0209</b><br><b>14.00</b> <b>Passcode: 072798</b>                               |
| 04                 | Zafer Demir<br>Turkey                                 | Parameters For Determining Policies And Targets For Heating And Cooling Systems in The Renewable Energy Power Sector |
| 05                 | Eduardo Erazo Acosta<br>Colombia                      | The Power of the Ancestral Philosophy of Sumak Kawsay  |
| 06                 | Dursun Aydın<br>Turkey                                | Nonparametric regression analysis based on Rational (Padé) approximation for censored-data                           |
|                    |   |  |

**20.08.2020 Thursday**

| ORAL PRESENTATIONS |  |   |
|--------------------|--|---|
|                    | <b>Chairing</b><br><b>Prof. Dr. Abidin Kılıç</b> | <b>Hall 1 Meeting ID: 986 0786 6678</b><br><b>15.00 Passcode: 221183</b>      |
| 07                 | Babaşova Əfşan Ağazayid<br>Qızı<br>Azerbaijan    | Aran İqtisadi-Coğrafi Rayonunda Şəhər Məskunlaşması və İnkişaf Perspektivləri |
| 08                 | Murat Başaran<br>Turkey                          | Gearbox Fault Classification by Using Frequency Based Feature Extraction      |
| 09                 | Christy A.A.<br>Norway                           | Comparison Of Desiccant Properties Of Natural Bio-Polymers                    |
|                    |  |   |

| ORAL PRESENTATIONS |   |   |
|--------------------|---|---|
|                    | <b>Chairing</b><br><b>Prof. Dr. Nihal Kuş</b> | <b>Hall 2 Meeting ID: 932 8681 0209</b><br><b>15.00 Passcode: 072798</b>            |
| 10                 | Ebru KOROGLU<br>Turkey                        | Antioxidant, Antibacterial, And Antiepileptic Potentials Of Some Pyrazine Compounds |
| 11                 | I.N.Askerzade<br>Azerbaijan                   | Iv Curve Of Josephson Junction With Majorana Term In Current-Phase Relation         |
| 12                 | Kevser Köklü<br>Turkey                        | Heavy Metal Analysis of The Ergene River, Turkey                                    |
|                    |   |   |

**20.08.2020 Thursday**

| ORAL PRESENTATIONS |  |  |
|--------------------|--|--|
|                    | <b>Chairing</b><br><b>Prof. Dr. Murad Omarov</b> | <b>Hall 1 Meeting ID: 986 0786 6678</b><br><b>16.00 Passcode: 221183</b>                                 |
| 13                 | Ömer Aydın<br>Turkey                             | Achieving Price and Performance Equality on and off The Grid by Examining Global Renewable Energy Trends |
| 14                 | Afamefuna Moon<br>Nigeria                        | A method for examining the sequencing models of symmetric structures                                     |
| 15                 | Fidan Veliyeva<br>Azerbaijan                     | The Effect of Colemanite Addition on The Microstructural And Mechanical Characteristics Of Ipp           |
| 16                 | Nihal Kuş<br>Turkey                              | Theoretical Analysis of The Structure Of Chiral Jasmonic Acid  |
|                    |  |  |

| ORAL PRESENTATIONS |   |  |
|--------------------|---|--|
|                    | <b>Chairing</b><br><b>Prof. Dr. Zafer Demir</b> | <b>Hall 2 Meeting ID: 932 8681 0209</b><br><b>16.00 Passcode: 072798</b>                             |
| 17                 | Sedef DİKMEN<br>Turkey                          | The Effect of Ionic Surfactants on The Zeta Potential Values of Talc A Naturally Hydrophobic Mineral |
| 18                 | Utku Kaya<br>Turkey                             | A Novel Color-Based Feature Extraction Method For Svm Based Skin Segmentation                        |
| 19                 | Mykola Moskalets<br>Ukraine                     | Experimental Studies of Video Content Transmission Characteristics in Adsl Subscriber Access Network |
| 20                 | Dursun Aydın<br>Turkey                          | Kernel Smoothing As an Imputation Technique for Right Censored Data                                  |
|                    |   |  |

**20.08.2020 Thursday**

| ORAL PRESENTATIONS |   |  |
|--------------------|---|--|
|                    | <b>Chairing</b><br><b>Prof. Dr. Zafer Demir</b> | <b>Hall 1 Meeting ID: 986 0786 6678</b><br><b>17.00 Passcode: 221183</b>   |
| 21                 | Fidan VELIYEVA<br>Azerbaijan                    | A Valuable View on Evaluation of General Mechanical Performances Pertaining To Bi-2223 Superconducting Ceramics with Vanadium Addition |
| 22                 | İman Askerzade<br>Azerbaijan                    | Influence of unconventional current-phase relation (CPR) on chaotic dynamics of Josephson junctions                                    |
| 23                 | Abidin Kılıç<br>Turkey                          | Determination of Approximate Crystal Size by HRXRD   |

| ORAL PRESENTATIONS |  |  |
|--------------------|--|--|
|                    | <b>Chairing</b><br><b>Prof. Dr. Dursun Aydın</b> | <b>Hall 2 Meeting ID: 932 8681 0209</b><br><b>17.00 Passcode: 072798</b>                   |
| 24                 | Zafer Dikmen<br>Turkey                           | Investigation of Ion Exchange and Magnetic Properties of Magnetically Modified Zeolite 13X |
| 25                 | Nihal Kuş<br>Turkey                              | Conformational Analysis Of Thiazole-5-Carboxylic Acid Using Dft/Td-Dft Methods             |
| 26                 | Nihal Kuş<br>Turkey                              | Natural Bond Orbital Interaction Analysis of Glycine                                       |
| 27                 | Ufuk Yıldız<br>Turkey                            | SUA Programming Language's Use in Turkey   |
|                    |  |  |

**21.08.2020 Friday**

| ORAL PRESENTATIONS |   |   |
|--------------------|---|---|
|                    | <b>Chairing</b><br><b>Prof. Dr. Nihal Kus</b> | <b>Hall 1 Meeting ID: 963 3611 3674</b><br><b>10.00 Passcode: 294914</b>  |
| 28                 | Saisha Saloni<br>India                        | Ammonia Adsorption Capacities of Natural Materials  |
| 29                 | Fidan Veliyeva<br>Azerbaijan                  | Examination of Vanadium Effect On General Mechanical Characteristics of Bi-2223 Materials Via Semi-Empiric Models |
| 30                 | Utku KAYA<br>Turkey                           | A Comparative Study Of Classification Methods On Human Skin Detection From Rgb And Ycbr Represented Color Images  |
|                    |   |   |

| ORAL PRESENTATIONS |  |  |
|--------------------|--|--|
|                    | <b>Chairing</b><br><b>Dr. Zafer Dikmen</b> | <b>Hall 2 Meeting ID: 926 9564 9701</b><br><b>11.00 Passcode: 492449</b>   |
| 31                 | Mohammad S.Al-Ajely<br>Iraq                | An efficient and solvent free synthesis of N-Aryl 2,3-dihydro-4H naphtho-[2,1-e] 1,3-oxazines                            |
| 32                 | Sedef Dikmen<br>Turkey                     | Adsorption of Some Anions by Sepiolite Belongs To Eskisehir (Sivrihisar) Region And Surface Active Agents-Modified Forms |
| 33                 | Nkiru E Ekechukwu<br>Nigeria               | A novel method for sperm quantification in the African malaria mosquito <i>Anopheles gambiae s.l</i>                     |
| 34                 | Abidin Kılıç<br>Turkey                     | Determination of Structural Defects of Superlattice Structures with HRXRD  |



**21.08.2020 Friday**

| <b>ORAL PRESENTATIONS</b> |  |   |
|---------------------------|--|---|
|                           | <b>Chairing</b><br><b>Prof. Dr. Abidin Kılıç</b> | <b>Hall 1 Meeting ID: 963 3611 3674</b><br><b>14.00 Passcode: 294914</b>  |
| 37                        | H.N. ADIGOZALZADE<br>Azerbaijan                  | Spectral Variability H $\beta$ Line of The Ae Herbig Type Star Hd 179218.   |
| 38                        | Sayyara Sadiqova<br>Azerbaijan                   | Eutectic Phase Crystallization in Co <sub>0,55</sub> Sb <sub>0,45</sub> -Sn and Co <sub>3</sub> Sn <sub>2</sub> -Sb Systems |
| 39                        | Menouar HANAFI<br>Algeria                        | The Bifunctional Catalyst Pt / Re Used in The Platforming Unit for Obtaining High Octane Number Of The Gasoline             |
| 40                        | Mykola PASTUSHENKO<br>Ukraine                    | Estimation of Mel-Frequency Cepstral Coefficients Using Phase Information of Voice Signal of Authentication System User     |

| <b>ORAL PRESENTATIONS</b> |   |   |
|---------------------------|---|---|
|                           | <b>Chairing</b><br><b>Dr. Utku Kaya</b> | <b>Hall 2 Meeting ID: 926 9564 9701</b><br><b>15.00 Passcode: 492449</b>  |
| 41                        | Liliya BATYUK<br>Ukraine                | The Effect Of Microwave Radiation of Low Intensity On Red Blood Cells At Ischemic Stroke  |
| 42                        | Maryna Yevdokymenko<br>Ukraine          | Investigation of The Qoe-Aware Adaptive Multipath Routing Model With Assurance of The R-Factor                                    |
| 43                        | Bala Ali RAJAVOV<br>Azerbaijan          | The Dark Matter And Energy in The De Sitter World   |
| 44                        | Olena CHALA<br>Ukraine                  | Mathematical Model Of The Development Of Manufacturing Defects In The Surface Layer Of Substrates Of Moems' Functional Components |

ISBN: 978-605-69034-6-5

# **ICONAT 2020**

**BAKU-AZERBAIJAN**

**AUGUST 20-22, 2020**

## **ABSTRACTS**

**Invited Speaker**  
Prof. Dr. Yüksel Ergün

## **Terahertz QWIP using Asymmetric Quantum Wells**

**M. Hostut<sup>1</sup>, T. Akın<sup>2</sup>, Y. Ergun<sup>3,2</sup>**

<sup>1</sup> Akdeniz uiversity, Dept Of Science Education/Antalya

<sup>2</sup> METU MEMS Center, METU Dept of Electric Electronic Engineering /Ankara

<sup>3</sup> Eskisehir Technical University, Dept of Physics/Eskisehir

As a well known photodetector, quantum well infrared photodetector (QWIP) design with containing multi-quantum well structures are highly desirable for terahertz range. These have potential applications such as imaging, material detection, and identification, a new generation of communication systems. The literature shows some QWIP structures utilizing single color, multicolor, broadband characteristics to reveal their characteristic potentials. For this reason we have designed asymmetric coupled quantum well structure in terahertz range. Band profile of the structure has been iteratively solved by Schrödinger–Poisson equation self-consistently. Intersubband energies are calculated by envelope function approximation (EFA) to obtain carrier wave functions. The asymmetric quantum wells contain three subband energy levels. Intersubband energy of ground to first subband and ground to second subbands are 7.7 and 15.9 meV corresponding to 1.86THz and 3.85THz respectively. Each period contains 60Å Al<sub>0.02</sub>Ga<sub>0.98</sub>As step layer followed by asymmetric coupled quantum wells with 200 and 70 Å undoped GaAs well layers separated by 50Å Al<sub>0.06</sub>Ga<sub>0.94</sub>As barrier layer. The step layer and the coupled QWs are sandwiched by two 800Å Al<sub>0.04</sub>Ga<sub>0.96</sub>As barriers. The bandstructure of the terahertz detector are shown in Fig. 1. The barriers are n-type doped (with Nd:3x10<sup>17</sup>cm<sup>-3</sup>) within 10 Å region away 10 Å from the barrier edge. This supplies electrons into the coupled QWs in order to eliminate the electron interactions with impurity atoms. The whole structure contains 30 periods of multi-quantum well structure structures (MQWs).

01

## **SOLUTION OF LOGARITHMIC KERNEL INTEGRAL EQUATIONS BY NATURAL TRANSFORM**

**Kevser KÖKLÜ<sup>1,\*</sup>, Erhan ÇALIŞKAN<sup>2</sup>**

<sup>1</sup> Department of Mathematical Engineering, Yildiz Technical University, İstanbul, Türkiye

<sup>2</sup> Institute of Science, Yildiz Technical University, İstanbul, Türkiye

### **ABSTRACT**

In this study, the resolvent of an integral equation was found with natural transform which is a new transformation which converged to Laplace and Sumudu transformations. At the same time, a solution to the first type of logarithmic kernel Volterra integral equations has been produced by the natural transform.

**Keywords:** Natural transform, solvent core (resolvent), logarithmic kernel, integral equations

02

## **KEYPOINT DETECTOR RETRAINING TECHNIQUES FOR THE COMMUNICATION SYSTEM OF SIGN LANGUAGE SPEAKERS**

**Guram CHAGANAVA, David KAKULIA**

Department of electric and electronic engineering, Faculty of exact and natural sciences, Ivane Javakhishvili Tbilisi State University, Tbilisi, Georgia

### **ABSTRACT**

The study described in this article examines the approaches of retraining of the deep learning model for hand palm keypoint detection in images. This is one of the studies conducted to create an innovative communication system for sign language speakers. The target of the given study is to find an optimal technique of retraining for increasing the degree of the keypoint detector generalization. So, it must be able to accurately detect keypoints in images it has not seen during training. It will make the communication system usable in real-life conditions.

In the article, there are reviewed three approaches of retraining: Retraining in series, retraining using united dataset and retraining using mixed datasets. Experiments were conducted to test the effectiveness of each of them. The paper presents the results of the experiments and a relatively optimal method selected among them.

ISBN: 978-605-69034-6-5

**Keywords:** Sign language. Communication system. Keypoint detection. Retraining.

## THEORETICAL AND EXPERIMENTAL VIBRATIONAL SPECTRUM ANALYSIS OF IONIC LIQUID 1-ETHYL-3-METHYLIMIDAZOLIUM CHLORIDE

Nihal KUŞ\* and Saliha ILICAN

Department of Physics, Science Faculty, Eskisehir Technical University,  
YunusEmre Campus, 26470 Eskisehir, Turkey

### ABSTRACT

A simple ionic liquids consist of an anions and cations. Anions are generally present in the small chain and in a larger form in the alkyl chain. In the present experimental study, 1-ethyl-3-methylimidazolium chloride in anion-cation form (EMIM-Cl) was studied both dispersed in KBr matrix and as a thin film. The studied ionic liquids were found to exhibit local environments in both the liquid and crystalline phases which are very similar. In both environments, the dominant forces are of Coulomb type, between the ions. Theoretical studies were undertaken at the DFT(B3LYP)/6-311++G(2d,2p) level of approximation using the GAUSSIAN 09 suit of program. EMIM cation has two conformers with minimum energy obtained by scanning the C-N-C-C dihedral angle.

**Acknowledgement:** This work was supported by the Eskisehir Technical University Commission of Research Project under grant no: 19ADP130.

**Keywords:** Ionic Liquids, Anion-Cation Pairs, 1-Ethyl-3-Methylimidazolium Chloride, Infrared Spectroscopy.

## PARAMETERS FOR DETERMINING POLICIES AND TARGETS FOR HEATING AND COOLING SYSTEMS IN THE RENEWABLE ENERGY POWER SECTOR

Ömer Aydın<sup>1</sup>, Zafer Demir<sup>2</sup>

<sup>1</sup>Graduate Education Institute, Eskisehir Technical University,  
Eskisehir, Turkey

<sup>2</sup>Porsuk Vocational School, Eskisehir Technical University,  
Eskisehir, Turkey

### ABSTRACT

Today there are various incentives for the use of renewable energy. We need to use these incentives to build our future at an optimum level. According to global data, a downward trend is observed in renewable energy-based heating and cooling systems. Legislation for heating and cooling in buildings need not be the primary objective to promote renewable energy generation and energy efficiency. Today, Europe is the most efficient continent in building energy efficiency. In particular, the use of renewable resources for heating comes to the forefront. Decarbonization in buildings is one of the leading studies in Europe and incentives are created and plans for the future are made. When we consider the industrial sector, it is observed that the dissemination and promotion activities in renewable energy heating and cooling systems are low. Countries should have a policy of increasing these incentives. This study covers the development of policies for renewable energy-based heating-cooling systems and plans made from past to present. In addition, the renewable energy-based heating-cooling sector will be examined and what needs to be done for the development of this sector will be examined.

05

## THE POWER OF THE ANCESTRAL PHILOSOPHY OF SUMAK KAWSAY (BUEN VIVIR) IN THE INDIGENOUS MOVEMENTS OF COLOMBIA

**Eduardo Erazo Acosta**

. Universidad de Nariño. Pasto - Nariño - Colombia.

### ABSTRACT

Ecuador vs. the exclusion by the big mining development, contribution to the Rights of Mother Nature from the global south.

The purpose of this research is to present the urgency of listening to indigenous epistemologies of *Sumak Kawsay* (in *kichwa* language: *Buen vivir*-Good Living) and also to accompany the care/defense of the biodiversity-rich indigenous territories of the Andean region. As a research question: How is the anthropocene affecting the indigenous territories and with it the threats of the epistemologies of *the Sumak Kawsay/Good Living*?

06

## Nonparametric regression analysis based on Rational (Padé) approximation for censored-data

Dursun Aydın<sup>1</sup> Ersin Yılmaz<sup>1</sup>

<sup>1</sup>: Mugla Sitki Kocman University, Faculty of Science, Department of Statistics, Mugla, 48000

### Abstract

This paper considers the estimation of a nonparametric regression model with randomly right-censored data. To estimate the model, rational (Padé) approximation based on truncated total least squares ( $P - TTLS$ ) is used as a smoothing method. Because of censored, data points cannot be used directly in modelling process, a data transformation is needed for overcoming this problem. As known, synthetic data transformation assigns censored points as zero and gives additional magnitudes to uncensored ones associated with Kaplan-Meier distribution of the censored dataset. Thus, the differences between censored and uncensored observations grow which causes a kind of spatial variation in the shape of data. In this paper, to bring a solution to this problematic situation,  $P - TTLS$  is used that works well on spatial variation. Also, to see the performance of the  $P - TTLS$  on censored data modelling, a simulation study is carried out and it is compared with the benchmarked kernel smoothing ( $B - KS$ ) method to observe how  $P - TTLS$  behaves.

## ARAN İQTİSADİ-COĞRAFI RAYONUNDA ŞƏHƏR MƏSKUNLAŞMASI VƏ İNKİŞAF PERSPEKTİVLƏRİ

Babaşova Əfşan Ağazayıd qızı  
Sumqayıt Dövlət Universiteti

### ABSTRACT

Məqalədə Aran iqtisadi-coğrafi rayonunun ayrı-ayrı şəhərləri üzrə əhali potensialı və sənaye istehsalının mövcud vəziyyəti araşdırılmışdır. İqtisadi-coğrafi rayonda məşğulluq və əmək resurslarından istifadə məsələsi araşdırılmaqla şəhərlərinin inkişaf perspektivləri şərh edilmişdir. Ətraf ərazilərin bol kənd təsərrüfatı xammalının tam, kompleks emalına əsaslanan müasir, rəqabətə dözümlü məhsul istehsal edə bilən müştərək (xarici investorları cəlb etmək hesabına) sənaye müəssisələrinin yaradılması Aran şəhərlərinin iqtisadi bazasını yaxşılaşdırır, sosial infrastrukturunu təkmilləşdirir. Aran iqtisadi-coğrafi rayonunun iqtisadi potensialı əsasında kənd təsərrüfatı və onunla əlaqədar emal, ticarət və sair sahələrinin inkişaf etdirilməsi artan demografik potensialı iş yerləri ilə təmin etməklə əhalisinin məşğulluq səviyyəsini yüksəldər və əhalinin yerlərdə qalmasını stimullaşdırar.

İqtisadi-coğrafi regionun bütün şəhər və qəsəbələrində demografik inkişafa uyğun sosial-iqtisadi inkişaf təmin olunmalı, ekoloji tarazlığın saxlanması, mühafizəsi və yaxşılaşdırılması daim diqqət mərkəzində olmalıdır. Yerli kənd təsərrüfatı xammalının kompleks emalına əsaslanan tam dövriyyəli, müasir standartlara uyğun məhsul istehsal edən əməktutumlu müəssisələrin inkişafı təmin edilməli, özəl sektorla yanaşı, dövlət müəssisələri də inkişaf etdirilməlidir. Pambıqtəmizləmə zavodlarında istehsal olunan məhsulün sapayırma, parçatoxuma, boyama, toxuma, tikiş mərhələlərini əhatə edən, müasir avadanlıqlarla təmin olunmuş kompleks yüngül sənaye müəssisələri nisbətən iri şəhərlərdə, ayrıca istehsal mərhələsini əhatə edən (məs. sapayırma, yaxud tikiş və s.) müəssisələri isə nisbətən kiçik şəhərlərdə yerləşdirmək olar. Belə müəssisələrin tikilməsinə ölkənin maliyyə durumu və daxili bazarda təbii məhsullara olan böyük tələbat da imkan verir və bunu zəruri edir.

## GEARBOX FAULT CLASSIFICATION BY USING FREQUENCY BASED FEATURE EXTRACTION

Murat BAŞARAN<sup>1\*</sup>, Mehmet FİDAN<sup>2</sup>

<sup>1,2</sup> Vocational School of Transportation, Eskişehir Technical University Eskişehir, Turkey

### ABSTRACT

Gearboxes are the fundamental elements of rotational systems to provide speed adjustment ratios from a rotating power source to another. In industrial applications, the existence of any kind of fault in rotational systems may be hazardous unless the early detection and maintenance procedures applied. Incipient types of faults such as a few chipped or worn teeth at the gearbox mechanism may deteriorate and cause the maladjustment of the rotation, even the mechanism may stop to rotate that may cause loss of the production. Preventive maintenance strategies such as monitoring the vibration signals and comparison of the frequency domain irregularities with normal operation case with healthy gearbox elements is essential to ensure safe and accurate rotational speed transmission in industrial systems. In this work, frequency domain characteristics of three different pinion conditions; healthy, a chipped tooth, and three consequent worn teeth are analyzed and frequency domain features are proposed for classification. Proposed features are classified with different classifiers and significant classification success observed with the proposed technique.

**Keywords:** Fault classification, fast fourier transform, gearbox, preventive maintenance



## COMPARISON OF DESICCANT PROPERTIES OF NATURAL BIO-POLYMERS

<sup>1</sup>Christy A.A., <sup>2</sup>Rathnaweera T.N., <sup>2</sup>Halanayake K.D.

<sup>1</sup>Department of Science, Faculty of Engineering and Science, University of Agder, Norway

<sup>2</sup>Department of Chemistry, Faculty of Science, University of Ruhuna, Matara, Sri Lanka  
[alfred.christy@uia.no](mailto:alfred.christy@uia.no), [thilininr315@gmail.com](mailto:thilininr315@gmail.com), [kalanadasunpriya@gmail.com](mailto:kalanadasunpriya@gmail.com)

### ABSTRACT

Desiccants are substances used in the dehumidification process which is vital in order to avoid the degradation of materials. Silica gel is the most prominent type of desiccant used and today the world has developed an interest in bio-polymers due to certain demerits of silica. Hence this study was conducted to investigate the desiccant properties of the four commercial flours wheat, corn, potato and gram and to compare them with the common silica gel desiccant. The bio-polymers were dried under vacuum at 120 °C and were studied over time using Near-Infrared (NIR) spectroscopy for their –OH combination peak which appears at around 5200 cm<sup>-1</sup> and the derivative spectra were analyzed to recognize the specific –OH groups involved in hydrogen bonding process. Further, the gravimetric analysis was used to study the rate of adsorption and their long-term efficacies were detected using data loggers.

The results clearly indicated that adsorption of water occurs at C1, C2+C3, C4 and C6-OH groups of the glucose units for wheat and corn flour while potato and gram flour showed only three peaks attributing to C1, C2+C3 and C6-OH. Further it was observed that C1 and C2+C3-OH groups have a similar and the highest rates. The rates of adsorption of all flours were greater than both analytical grade and commercial silica and corn flour was found to be an outstanding desiccant compared to conventional silica desiccant.

**Keywords:** Adsorption, bio-desiccant, Near-Infrared (NIR) spectroscopy, Gravimetric

## ANTIOXIDANT, ANTIBACTERIAL, AND ANTIEPILEPTIC POTENTIALS OF SOME PYRAZINE COMPOUNDS

Ebru KOROGLU<sup>1\*</sup>, Hasan Ufuk CELEBIOGLU<sup>1</sup>, Recep TAŞ<sup>1</sup>, Parham TASLIMI<sup>1</sup>, Nina LADOCHINA<sup>2</sup>, Afsun SUJAYEV<sup>2</sup>

<sup>1</sup>Department of Biotechnology, Faculty of Science, Bartın University, 74100 - Bartın, Turkey

<sup>2</sup>Laboratory of Faine Organic Synthesis, Institute of Chemistry of Additives, Azerbaijan National Academy of Sciences, 1029 Baku, Azerbaijan

### ABSTRACT

Pyrazines are a class of compounds found almost everywhere in nature and can be synthesized chemically or biologically. People take pyrazines from their main source of nutrients. Pyrazines are detected in heated foods, such as cocoa, peanuts, coffee, popcorn, beef products, fried barley; as well as fresh foods, such as green peppers, tomatoes, peas, and dairy products (1). Pyrazines are produced not only in heated foods but also in fermented foods during the fermentation process (2).

Microorganisms are the oldest living things on earth and have ability to adapt quickly to changing conditions (3). Every new microorganism that developed with these capabilities finds a way to escape antibiotics. As a result, the resistance problem arises in antibiotics which is the most important obstacle in the fight against infections. Antibiotic resistance is that some strains of a species are not affected by antibiotics, or getting resistant by various resistance mechanisms. Acquired antibiotic resistance is caused by mutations in the

chromosomes of microorganisms or by transferring the resistance gene of a resistant microorganism to the susceptible microorganism. Antibiotic resistance in microorganisms is increasing due to increased consumption of antibiotics in the community, increased number of immunocompromised patients, and antibiotic use in the food industry. *Shigella* spp., *Neisseria gonorrhoeae*, *Escherichia coli*, and *Staphylococcus aureus* are among the most resistant microorganisms (4-6). Antimicrobial tests are used against gram positive, gram negative bacteria and fungi to determine whether the compounds show antimicrobial properties.

Furthermore, the antioxidant activity of a compound can be determined by using DPPH (diphenyl-1-polyhydrazil. DPPH is a stable organic nitrogen radical obtained commercially.

Carbonic anhydrase (hCA; E.C.4.2.1.1) plays a role in the accumulation of  $H^+$  and  $HCO_3^-$  in many tissues as well as providing metabolic  $CO_2$  transport in general. CA I, II and III, three of the sixteen known isoenzymes of carbonic anhydrase, were crystallized and very detailed information about the structures of these isoenzymes was determined. These three important isoenzymes are also dissolved in the cytoplasm of the cells (7). Inhibitors of these isoenzymes are extremely important for epilepsy studies.

Thus, the aim of the present study is to investigate antibacterial, antioxidant, and antiepileptic properties of newly synthesized pyrazine compounds, (1-(phenylsulfonyl)-1,3a-dihydropyrazolo[1,5-a]pyridin-3-yl)methanol (T63) and 2-methyl-1-(phenylsulfonyl)-1,2,3,3a-tetrahydropyrazolo[1,5-a]pyridin-3-ol (T70).

A new method of obtaining multifunctional pyrazoles by the reaction of 1,3-dipolar addition of tribenzylsulfonyliminochloride to polarophiles has been developed. This imine is obtained by reacting tribenzylamine with N-chlorobenzene sulfamide (chloramine-B). Regardless of the structure and composition of polarophiles, the cyclization reaction takes place in the presence of alkali in 6-8 hours of boiling, which proves the activation of the methylene groups of tribenzylamine using the electron-withdrawing sulfonamide group.

Different concentrations (0-125  $\mu\text{g/mL}$ ) of T63 and T70 were used for antibacterial test against *E. coli* and *S. aureus*. Around %10 inhibition of *E. coli* viability, %10-13 inhibition of *S. aureus* were observed at 125  $\mu\text{g/mL}$ . Furthermore, no significant antioxidant activity was observed for any of two compounds.

$K_i$  values for hCA I isoenzyme of these two compounds were obtained at  $874.30 \pm 57.27$  and  $688.04 \pm 84.11$   $\mu\text{M}$ , respectively. For hCA II,  $K_i$  values were  $780.40 \pm 65.41$  and  $607.55 \pm 35.98$   $\mu\text{M}$  respectively.

In conclusion, the present study gives insight into biological activities of novel pyrazine compounds, (1-(phenylsulfonyl)-1,3a-dihydropyrazolo[1,5-a]pyridin-3-yl)methanol (T63) and 2-methyl-1-(phenylsulfonyl)-1,2,3,3a-tetrahydropyrazolo[1,5-a]pyridin-3-ol (T70).

**Keywords:** Pyrazines; antimicrobials; carbonic anhydrase; enzyme inhibition; antioxidant

## REFERENCES

- 1) Maga JA, Sizer CF (1973) Pyrazines in foods. A review. J Agric Food Chem 21:22–30
- 2) Besson I, Creuly C, Gros JB, Larroche C (1997) Pyrazine production by *Bacillus subtilis* in solid-state fermentation on soybeans. Appl Microbiol Biotechnol 47:489–495
- 3) Vahaboğlu H. Antibiyotiklerde direnç sorunu. Türkiye Klinikleri Farmakoloji Özel,2004; 2: 92-96.
- 4) Töreci K. Antibiyotik kullanımı ve direnç ilişkisi. Flora 2003; 8: (2): 89-110.
- 5) Gold HS, Moellering Jr RC. Antimicrobial-drug resistance. The N Engl J Med, 1996; 335 : 1445-1451.
- 6) Archibald L, Phillips L, Monnet D, McGowan JE Jr, Tenover F, Gaynes R. Antimicrobial resistance in isolates from inpatients and outpatients in the United States: Increasing importance of the intensive care unit. Clin Infect Dis, 1997; 24: 211-5.
- 7) Biçer A, Taslimi P, Yakalı G, Gülçin İ, Gültekin MS, Cin GT. (2019). Synthesis, Characterization, Crystal Structure of Novel Bis-Thiomethylcyclohexanone Derivatives and Their Inhibitory Properties Against Some Metabolic Enzymes. Bioorganic Chemistry, 2019; 82: 393-404.

## IV CURVE of JOSEPHSON JUNCTION with MAJORANA TERM in CURRENT-PHASE RELATION

I. N. ASKERZADE<sup>a,b</sup>, N. KARTLI<sup>a</sup>, H. B. YILDIRIM<sup>a</sup>,

<sup>a</sup>Department of Computer Engineering and Center of Excellence of Superconductivity Research, Ankara University, Ankara, 06100, Turkey

<sup>b</sup>Institute of Physics Azerbaijan National Academy of Sciences 33, H.Cavid 33. Baku, AZ1143, Azerbaijan

In this study we carried out the analysis of the influence of unconventional current-phase relation on IV curve of single Josephson junction. In the case of Josephson junctions on topological superconductors, the current-phase relation include additional fractional term [1-2],

$$I = I_c f_m(\phi) = I_{c0}(\sin \phi + m \sin(\phi/2)) \quad (1)$$

Second term in Eq. (1) related with Majorana quasi-particles and dynamical detection of this particles seems very challenging in solid state physics. Discovery of Majorana fermions seems interesting from the point of fault-tolerant quantum computing [3]. Some dynamical properties of Josephson junction with unconventional current-phase relation  $I = I_{c0}(\sin \phi + \alpha \sin(2\phi))$  was investigated in Ref. [4]. In this study we carried out the analysis of IV curve of the single junction with unconventional relation (1). The dynamics of Josephson junction for the case of current-phase relation (1) is given by the equation of resistive model [4]

$$\beta \ddot{\phi} + \dot{\phi} + f_m(\phi) = i_e \quad (2)$$

where  $i_e$  external dc current in units of critical current  $I_c$ , dots over  $\phi$  corresponds to derivative

in respect to dimensionless time  $\frac{\Phi_0}{2\pi I_c R_N}$ ,  $\Phi_0$  is the magnetic flux quantum.  $\beta$  is the McCumber

parameter of Josephson junction  $\beta = \frac{2e}{\hbar} I_c R_N^2 C$ , which determine the size of hysteresis in IV curve.

The numerical solution of Eq. (1) will be obtained using Runge-Kutta four order method. For average voltage we use the time averaging procedure of numerical solution. IV curve will be presented for different amplitude of Majorana term  $m$  and McCumber parameter  $\beta$ .

This study supported by TÜBİTAK grant 118F093.

### References

1. Maiti M.L. et al , Phys Rev B,92,224501(2015)
2. Kulikov K. at al, JETP,125,333(2018)
3. Wendin G, Reports on Progress in Physics,80,106001(2017)
4. Askerzade I, Bozbey A., Canturk M., Modern aspects of Josephson Dynamics and superconductivity electronics, Springer, Berlin, 2017,210 p.

**HEAVY METAL ANALYSIS OF THE ERGENE RIVER, TURKEY**

Kevser KÖKLÜ<sup>1</sup>, Arda BENZET<sup>2</sup>, Asude KÖKLÜ<sup>3</sup>, Sinan Koca<sup>2</sup>, Betül Oyku Ozguven<sup>2</sup>, Azra Gurer<sup>2</sup>, Elif Nas Dereli<sup>2</sup>, Ecenaz Ozer<sup>2</sup>, Alper Benzet<sup>2</sup>, Erdener Tuna Aytekin<sup>2</sup>, Umut Sarp Aygun<sup>2</sup>, Deniz Can<sup>2</sup>, Yaprak Basaran<sup>2</sup>, Hatice Benzet<sup>4</sup>

<sup>1</sup> Department of Mathematical Engineering, Yıldız Technical University, İstanbul, Türkiye

<sup>2</sup> Kırklareli Science High School, 39000, Kırklareli, Türkiye

<sup>3</sup> Hüseyin Avni Sözen Anatolian High School, İstanbul, Türkiye

<sup>4</sup> Kırklareli Genç Gelecek Private Education Institutions, 39000, Kırklareli, Türkiye

**ABSTRACT**

The study focuses on the *Ergene River* Basin. The river faces a significant contamination problem because it flows through the industrial intensive industrial zone. Almost all industrial, domestic, and agricultural wastewater is discharged directly or indirectly to the Ergene River. With this discussion, eight heavy metal analysis of samples collected from thirteen different points of the river is introduced. The discussion begins with descriptive analysis, binary correlations, and hierarchical cluster analysis of eight heavy metals. The explain percentages of the three eigenvalues and the correlation matrix continue with linear modeling by clustering the variables. It discusses with the *Contamination Factor* (CF), *Enrichment Factor* (EF), and *Pollution Load Index* (PLI) values to get to reveal the *anthropogenic* effect more closely.

**Keywords:** Ergene River, contamination factor, enrichment factor, pollution load index.

**ACHIEVING PRICE AND PERFORMANCE EQUALITY ON AND OFF THE GRID BY EXAMINING GLOBAL RENEWABLE ENERGY TRENDS,**

Ömer Aydın<sup>1</sup>, Zafer Demir<sup>2</sup>

<sup>1</sup>Porsuk Vocational School, Eskisehir Technical University, Eskisehir, Turkey

<sup>2</sup>Graduate Education Institute, Eskisehir Technical University, Eskisehir, Turkey

**ABSTRACT**

Renewable energy sources are an increasing trend in the world as an alternative solution to rapidly depleting fossil fuels. Other reasons for preference are that these resources are cost-effective and environmentally friendly. Increasing importance of governments' support for the development of renewable energy technologies and consequently the development of these energy technologies is one of the most important steps in the world. Among the renewable energy sources, solar and wind power plants, which are the most popular ones, decrease the electricity prices compared to the companies that produce high-priced electricity with non-renewable energy sources. When we think about it, for consumers who apply 3-time tariff, solar energy provides price regulation during the day and wind energy reduces the costs by night price regulation. In order for this system to be an uninterruptible power supply, its operation as a hybrid affects supply security and energy quality positively. In countries with high levels of development, it is possible to see that the most popular wind and solar energy price balance among renewable resources and the cost difference between these and other generations of resources are increasing all over the world. In order to achieve price and performance equality on and off the grid, we will review the global renewable energy trends and explain what needs to be done.

**Key words:** Hybrid systems, renewable energy, energy sources, price and performance equality, energy trends

14

**A METHOD FOR EXAMINING THE SEQUENCING MODELS OF SYMMETRIC STRUCTURES**

Afamefuna Moon  
Federal University, Nigeria

**ABSTRACT**

Some Symmetric protein assemblies get important roles in many biochemical processes. This study for application of a general framework for modeling arbitrary symmetric systems. The various types of symmetries was described in this study. Because of the symmetric modeling capabilities was run simulations on symmetric systems.

15

**THE EFFECT OF COLEMANITE ADDITION ON THE MICROSTRUCTURAL AND MECHANICAL CHARACTERISTICS OF IPP**

Ugur SOYKAN<sup>1,\*</sup>, Fidan VELIYEVA<sup>2</sup>

<sup>1</sup>Yenicaga Yasar Celik Vocational High School, Bolu Abant Izzet Baysal University, Bolu-Turkey

<sup>2</sup>Department of Chemistry, Bolu Abant Izzet Baysal University, Bolu-Turkey  
e-mail of the corresponding author: [ugursoykan@ibu.edu.tr](mailto:ugursoykan@ibu.edu.tr)

**ABSTRACT**

The objective of this study was to investigate the effect of the addition of the colemanite having 45 $\mu$ m size on the significant characteristic features of the isotactic polypropylene (IPP). The microstructural properties (diffraction pattern,  $a$ ,  $b$  and  $c$  unit cell parameters and grain size) and mechanical behaviors (tensile strength, Young's Modulus, impact strength and percent elongation) of the samples relative to the colemanite content (5, 10, 15, 20 and 30 wt.%) were studied in details. The optimum amount of colemanite content was determined for IPP based composites having the improved properties. The obtained samples were characterized by using XRD technique and the conventional mechanical tests. The results showed that the content level of the colemanite considerably affected to the fundamental properties of IPP. As for microstructural properties, it was observed from the XRD patterns that all composite samples mainly showed both  $\alpha$  form (monoclinic arrangement) and  $\beta$  form (hexagonal arrangements) in the crystalline domains. Moreover, the finding revealed that  $a$  and  $b$  the unit cell parameters of IPP based composites increased initially, reached the maximum values with the products containing 10% of colemanite, and then the consistent decrement trend was observed with the further increasing of the colemanite content in the products. Furthermore, the mechanical test measurements depicted that the reinforcements were achieved in the tensile, Modulus and impact strengths of the composite materials, while the percent elongation of the products decreased with the increasing of the colemanite content. 7.4%, 24.9% and 6.7% increases were recorded in the tensile strength, Modulus and impact strength at the product with 10% colemanite, respectively. The improvements was probably stemmed from that the presence of micro size colemanite particles gave rise to increment in the orientations and alignments of IPP chain in the matrix.

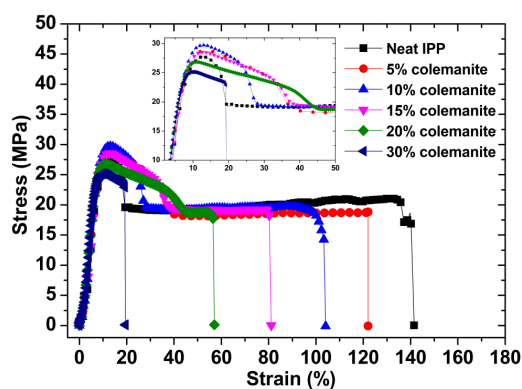


**Figure 1.** Strain-stress curve of neat IPP and IPP based composites with the content of 5, 10, 15, 20 and 30% colemanite.

**Key words:** colemanite, unit cell parameters, mechanical properties, IPP based composites, percent elongation.

16

## THEORETICAL ANALYSIS OF THE STRUCTURE OF CHIRAL JASMONIC ACID

Nihal KUŞ

Department of Physics, Science Faculty, Eskisehir Technical University,  
YunusEmre Campus, 26470 Eskisehir, Turkey

### ABSTRACT

Jasmonic acid (JA), a molecule formed by the oxygenation of fatty acids, is an organic compound and is found in many plants, especially jasmine. The conformation of this compound is found according to the location in the chiral centers. In this study, the molecular structure of JA, which has two chiral centers in C-4 and C-5 (labeled in this study), was investigated by DFT and TD-DFT methods. These structures have been found to have RR, RS and SS configurations relative to their chiral centers. Each configuration has *cis* and *trans* conformations depending on the orientation of the chain groups attached to the five atom ring. The minimum energies of each conformation were calculated using DFT/B3LYP/6-311++G(d,p) method and the structures of their stable form were drawn. JA\_RR\_trans (Fig.1) conformer was found most stable than the other conformers. Excited state energies were calculated using TD-DFT calculations and also HOMO-LUMO energy gaps were found for all chiral conformers.

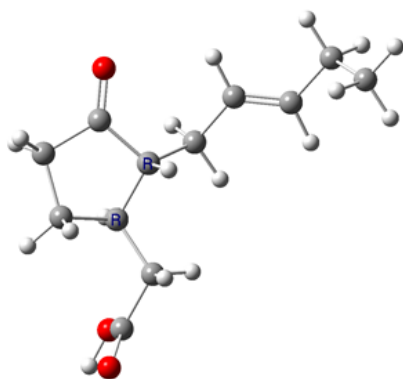


**Fig.1.** JA\_RR\_trans conformer calculated at the B3LYP/6-311++G(d,p) level of approximation

**Keywords:** Jasmonic acid, chiral, DFT, TD-DFT, NBO, HOMO-LUMO.

## THE EFFECT OF IONIC SURFACTANTS ON THE ZETA POTENTIAL VALUES OF TALC A NATURALLY HYDROPHOBIC MINERAL

Sedef DİKMEN<sup>1</sup>, Bahri ERSOY<sup>2</sup>

<sup>1</sup> Department of Physics, Faculty of Science, Eskişehir Technical University, Eskişehir, Turkey

<sup>2</sup> Mining Engineering Department, Faculty of Engineering, Afyon Kocatepe University, 03200, Afyonkarahisar, Turkey

### ABSTRACT

In the present work, a comparative study on the adsorption mechanisms of three kinds of surfactants which are cationic (hexadecyltrimethylammonium bromide, HTAB), anionic (sodium dodecyl sulphate, SDS) and non-ionic (Triton X-100, TX-100) onto talc were carried out. In this scope, a series of batch adsorption tests, zeta potential (ZP) measurements, infrared spectroscopy (FT-IR) studies, thermogravimetric (TG) analysis were performed. The amount of maximum adsorption of the surfactants onto talc are ordered as in the following: TX-100 ( $\sim 9 \times 10^{-5}$  mol/m<sup>2</sup>) > HTAB ( $\sim 8 \times 10^{-5}$  mol/m<sup>2</sup>) > SDS ( $\sim 5 \times 10^{-5}$  mol/m<sup>2</sup>). Even though both the SDS and talc have negative surface charge, SDS can adsorb onto talc. Moreover, a good correlation has been seen between the adsorption isotherms and the zeta potential curves. Considering their adsorption isotherms, the ionic surfactants show different adsorption behavior concerning the non-ionic surfactant molecules. That is, the adsorption isotherm of HTAB and SDS increase rapidly in a narrow concentration range until the plateau region (max adsorption density), while such a sharp increase does not appear for TX-100. In contrast, the maximum adsorption amount of TX-100 is greater than those of SDS and HTAB. The results indicate that hydrophobic interaction and hydrogen bonding play a decisive role on the adsorption of non-ionic and anionic surfactants onto talc a naturally hydrophobic mineral, whereas electrostatic interaction becomes more important in the adsorption of cationic surfactant.

**Keywords:** Adsorption, FT-IR, Surfactant, Talc, Zeta Potential

## A NOVEL COLOR-BASED FEATURE EXTRACTION METHOD FOR SVM BASED SKIN SEGMENTATION

Mehmet FİDAN<sup>1,\*</sup>, Utku KAYA<sup>2</sup>

<sup>1</sup> Vocational School of Transportation, Eskişehir Technical University Eskişehir, Turkey

<sup>2</sup> Vocational School of Transportation, Eskişehir Technical University Eskişehir, Turkey

### ABSTRACT

The colored digital images can be represented in different color spaces. The most used color space is Red-Green-Blue space. However, this space can be transformed to Luminance-Blue Difference-Red Difference space for extraction of light intensity information and Hue-Saturation-Value space. The defined features of color pixels give strong information about whether they belong to a human skin or not. In this paper, a novel color-based feature extraction method is proposed, which use both red, green, blue, luminance, hue and saturation information. The proposed method is applied on an image database consists of various people with diverse age, racial and gender characteristics. The obtained features are used to segment the human skin by using Support-Vector- Machine algorithm and finally the promising performance results are presented comparatively with the most-common methods in the literature.

**Keywords:** Feature extraction, Image segmentation, Support Vector Machine,

## EXPERIMENTAL STUDIES OF VIDEO CONTENT TRANSMISSION CHARACTERISTICS IN ADSL SUBSCRIBER ACCESS NETWORK

AL-VANDAVI SAIF AHMED ISKANDAR ISMAEL<sup>1</sup>, Mykola MOSKALETS<sup>2</sup>, Kostiantyn SIELIVANOV<sup>3</sup>, Hvostyk IHOR<sup>4</sup>

V.V. Popovskyy Department of Infocommunication Engineering,  
Kharkiv National University of Radio Electronics  
Nauky Ave. 14, Kharkiv, Ukraine  
mykola.moskalets@nure.ua

**Abstract.** The dependences of the video stream rate on the frame rate were experimentally obtained using standard and high definition video files and the corresponding H.264 codec profiles. A machine experiment was carried out to confirm the performance of the proposed model, for which the least squares methods were used and the confirming coefficients were obtained. Using the developed technique, the experimental dependences were approximated by the least squares method, and for each of them the corresponding coefficients of the approximating polynomials of the  $n$ th degree were obtained. Subsequently, these coefficients were used by the video quality assessment function for subjective assessment of the integral quality of multimedia. An experimental evaluation of the performance of ADSL/2/2+ systems for the entire range of linear DSLAM rates for video content transmission has been carried out. The experimental results are compared with the calculated values using a multi-layer model for assessing the performance and quality of multimedia. The calculation method and the results of the work can be used to implement IPTV in real access networks based on ADSL2 + technology.

### REFERENCES

- [1] ITU-T Recommendation H.264 (03/2009) - Advanced video coding for generic audiovisual services.
- [2] ITU-T Rec. G.992.1 Asymmetric digital subscriber line (ADSL) transceivers. International Telecommunication Union. 1999. P.256.
- [3] DSL Forum TR-017 ATM over ADSL Recommendation / The Broadband Forum. 1998. P.33.
- [4] ATIS-0800004 A Framework for QoS Metrics and Measurements Supporting IPTV Services. 2006.
- [5] ITU-T Recommendation G.107 The E-model: a computational model for use in transmission planning. 2011. P.26.
- [6] ITU-T Recommendation Y.1910 IPTV functional architecture. 2008. P.102.
- [7] ITU-T Recommendation Y.1911 IPTV services and nomadism: Scenarios and functional architecture for unicast delivery. 2010. P.26.
- [8] ITU-T Recommendation Y.1991 Terms and definitions for IPTV. 2010. P.28.
- [9] Lawson C.L., Hanson R.J. Solving Least Squares Problems. Revised republication. — Society for Industrial and Applied Mathematics, 1995. — 352 p.
- [10] ISO/IEC 14496-10 Information technology Coding of audio-visual objects Part 10: Advanced Video Coding. – 2009.



## KERNEL SMOOTHING AS AN IMPUTATION TECHNIQUE FOR RIGHT-CENSORED DATA

Dursun Aydın<sup>1</sup> Ersin Yılmaz<sup>1</sup>

<sup>1</sup> Mugla Sitki Kocman University, Faculty of Science, Department of Statistics, Mugla, 48000

### Abstract

Imputation of right-censored observations has crucial importance in statistical and other fields of science. Because of right-censored datasets are encountered commonly in medical studies and survival analysis, researchers have to be more meticulous about data quality. Thus, imputation techniques are used to complete the censored data points by estimating them correctly. This study introduces the kernel smoothing method as an imputation technique for taking account of the structure of the data and individuals effects of data points that can be achieved by kernel weights. Fundamental idea is to obtain a nonparametric model from the incomplete dataset and making in-sample predictions to estimate censored ones. In order to show benefits of the method, a simulation study is carried out and it is also compared by Ordinary least squares (OLS) based imputation which is one of the widely used imputation methods and works similar to the proposed method.

## A VALUABLE VIEW ON EVALUATION OF GENERAL MECHANICAL PERFORMANCES PERTAINING TO BI-2223 SUPERCONDUCTING CERAMICS WITH VANADIUM ADDITION

Ugur SOYKAN<sup>1,\*</sup>, Fidan VELIYEVA<sup>2</sup>, Gurcan YILDIRIM<sup>3</sup>

<sup>1</sup>Yenicaga Yasar Celik Vocational High School, Bolu Abant Izzet Baysal University, Bolu-Turkey

<sup>2</sup>Department of Chemistry, Bolu Abant Izzet Baysal University, Bolu-Turkey

<sup>3</sup>Bolu Abant Izzet Baysal University, Department of Mechanical Engineering, Bolu-Turkey

e-mail of the corresponding author: [ugursoykan@ibu.edu.tr](mailto:ugursoykan@ibu.edu.tr)

### ABSTRACT

In this research, our scientific group investigates the effect of vanadium addition in the Bi-2223 superconducting matrix on the general mechanical performance features by the help of experimental microhardness measurements conducted by a small indenter between the well-defined stress loads of 0.245 N and 2.940 N. Moreover, we determine the key mechanical design parameters including the elastic moduli with the hardness, stiffness coefficients, fracture toughness, yield strength, brittleness index and its opposite behavior (ductility) in the applied test loads given using the experimental data deduced from the microindentation tests. According to the experimental findings, it is observed that the presence of vanadium content in the Bi-2223 crystal structure surpasses seriously the general mechanical performance and related parameters due to the degradation in the quality of grain boundary couplings, crystal structure and basic structural quantities as a consequence of the increment in the structural problems, permanent plastic deformations, crack-producing flaws and dislocations. In other words, the augmentation of vanadium compounds in the Bi-2223 superconducting lattice brings about the considerable enlargement in the responsibility to the static indentation loads. Namely, the sensitive level to the applied loads increases rapidly with the vanadium concentration. We also search the variation of graphs between the Vickers hardness parameters and applied test loads. In this respect, all the materials prepared in this work exhibit the standard

ISE (indentation size effect) characteristics but within the decrement trend as the vanadium content level increases. In more detail, the impurity atoms damage harshly the ISE feature of Bi-2223 type-II superconducting ceramics. Additionally, we discuss the change of plateau limit regions coincided with the permeant artificial structural problems in the graphics. The vanadium leads to shorten the applied test load values for the plateau limit regions of Bi-2223 materials, stemmed from the enhancement the general structural problems. To conclude, the vanadium inclusions are ploughed to improve the general mechanical performance features and key mechanical design parameters.

**Keywords:** Vanadium added Bi-2223 material; Microindentation tests; General mechanical performance features; ISE feature.

## 22

### INFLUENCE OF UNCONVENTIONAL CURRENT-PHASE RELATION (CPR) ON CHAOTIC DYNAMICS OF JOSEPHSON JUNCTIONS

I.N.ASKERZADE<sup>a,b</sup>, N.KARTLI<sup>a</sup>, H.B.YILDIRIM<sup>a</sup>,

<sup>a</sup>Department of Computer Engineering and Center of Excellence of Superconductivity Research, Ankara University, Ankara, 06100, Turkey

<sup>b</sup>Institute of Physics Azerbaijan National Academy of Sciences 33, H.Cavid 33. Baku, AZ1143, Azerbaijan

The literature has shown that many simple nonlinear systems, including Josephson circuits, can exhibit chaotic dynamics. In this manner, Josephson junction devices could be useful for ultrahigh-speed chaotic generators for applications of code generation in spread-spectrum communications and true random number generation in secure communication and encryption. From this point of view, the dynamics of Josephson junctions is of great importance.

In the case of Josephson junctions on topological superconductors and new superconductors, CPR include additional term [1-3],

$$I = I_c f_{m,\alpha}(\phi) = I_{c0} \begin{cases} (\sin \phi + m \sin(\phi/2), \text{Majorana ... case} \\ (\sin \phi + \alpha \sin(2\phi)), \text{anharmonic ... case} \end{cases} \quad (1)$$

The influence of second term of CPR on an externally shunted Josephson junction on chaotic dynamics using circuit model with nonzero inductance has been studied. Using the circuit model, the time dependent simulations are carried out for a variety of control parameters. It is shown that the presence of second term on CPR leads to a change in the boundary of the chaotic region in bifurcation diagram. The bifurcation dynamics of Josephson junction for the case of CPR (1) is given by the equation of resistive model

$$\beta \ddot{\phi} + \dot{\phi} + f_{m,\alpha}(\phi) = i_e \quad (2)$$

where  $i_e$  external dc current in units of critical current  $I_c$ , dots over  $\phi$  corresponds to derivative in respect to dimensionless time  $\frac{\Phi_0}{2\pi I_c R_N}$ ,  $\Phi_0$  is the magnetic flux quantum.  $\beta$  is the McCumber parameter of Josephson

junction  $\beta = \frac{2e}{\hbar} I_c R_N^2 C$ . The numerical solution of Eq. (2) obtained using Runge-Kutta four order method.

This study supported by TÜBİTAK grant 118F093.

#### References

1. I.Askerzade, A. Bozbey, M. Canturk, 2017. Modern aspects of Josephson Dynamics and superconductivity electronics, (Springer, Berlin), 2017
2. M.L.Maiti et al, Phys Rev B, 92, 224501 (2015)
3. K. Kulikov et al, JETP, 125, 333 (2018)

## 23

## **DETERMINATION OF APPROXIMATE CRYSTAL SIZE BY HRXRD**

Abidin Kılıç

Physics Department, Faculty of Science, Eskisehir Technical University, Eskisehir- Turkey

### **ABSTRACT**

X-ray reflectivity (XRR) measurement is not a technique for evaluating diffraction phenomena. The XRR measurement technique is used to analyze X-ray reflection intensity curves from grazing event to X-ray beam to determine thin film parameters including thickness, density and surface or interface roughness. It will provide an overview of X-ray reflection principles, measurement procedures and analysis methods. It also discusses planned workflow and measures from measurement to analysis. In this study, a general evaluation will be made about measurement techniques.

**24**

## **INVESTIGATION OF ION EXCHANGE AND MAGNETIC PROPERTIES OF MAGNETICALLY MODIFIED ZEOLITE 13X**

Zafer Dikmen

Physics Department, Faculty of Science, Eskisehir Technical University, Eskisehir- Turkey

### **ABSTRACT**

The literature review, which we have done up to now, shows that there is no study about magnetic modification process for 13X zeolite or that we haven't found one even if there were one. For this reason, this study was realized on magnetic modified 13X zeolite about magnetically modification by using magnetite obtained from Divrigi region Turkey. After modification process, samples were characterized by XRD, XRF, SEM, EDX, VSM. Then, ion exchange and magnetic properties of unmodified and modified zeolites were compared with each other. According to these findings, modified zeolites have better ion exchange and magnetic properties than the other's.

## CONFORMATIONAL ANALYSIS OF THIAZOLE-5-CARBOXYLIC ACID USING DFT/TD-DFT METHODS

Nihal KUŞ

Department of Physics, Science Faculty, Eskisehir Technical University,  
YunusEmre Campus, 26470 Eskisehir, Turkey

### ABSTRACT

In this work, structures of the conformations of the thiazole-5-carboxylic acid (T5CA) were studied using density functional theory (DFT) with B3LYP/6-311++G(d,p) level of approximation. From calculations of the potential energy distribution depending on the orientation of the carboxylic acid group (C-C-OH and O = C-OH) attached to the five-membered heterocyclic ring, four conformers were found at minimum energy. Considering that the relative energy in the most stable structure is zero, (T5CA\_1; Fig.1) the relative energies of the other conformations were found to be about 0.14, 27.11, 29.84 kJ mol<sup>-1</sup>, respectively. It was found that the carboxylic acid group of the T5CA\_3 and 4 were not planar, while T5CA\_1 and 2 were planar. Stabilization and donor-acceptor orbital interaction energies were calculated for all conformations and orbitals were plotted using natural bond orbital analysis (NBO) method. The excited state energies were calculated and graphed using Time-Dependent Density Functional Theory (TD-DFT) calculations. The singlet state energies were tabulated for all conformations and it was seen that the most stable form with the highest oscillator strength was at the second singlet state (S<sub>2</sub>). In addition, HOMO-LUMO energy gaps were calculated and electrostatic potential surface maps were drawn for all conformations.

## NATURAL BOND ORBITAL INTERACTION ANALYSIS OF GLYCINE

Saliha ILICAN

Nihal KUŞ

Department of Physics, Science Faculty, Eskisehir Technical University,  
YunusEmre Campus, 26470 Eskisehir, Turkey

### ABSTRACT

In this study, the glycine (*Gly*; C<sub>2</sub>H<sub>5</sub>NO<sub>2</sub>) molecule was theoretically analyzed using natural bond orbital (NBO) interactions with DFT/B3LYP/6-311++G(d, p) method. All calculations were performed for three main conformers with minimum energy state. Donor-acceptor interactions of *Gly* were calculated using second order Fock matrix Schrödinger equation. Effects of bond polarization and hybridization were analyzed in wave functions associated with the formation of conformers. The global reactivity descriptors such as electronegativity ( $\chi$ ), electronic potential ( $\mu$ ), hardness ( $\eta$ ), softness ( $\sigma$ ) and global electrophilicity index ( $\omega$ ) were calculated for three main conformers of *Gly*. The molecular electrostatic potential (MEP) energy surfaces of the molecule allow us to identify charged regions that vary in a molecule. MEP surfaces were plotted for three main conformers of *Gly* molecule calculated by density functional theory with B3LYP/6-311++G(d, p) level.

**Acknowledgement:** This work was supported by the Eskisehir Technical University Commission of Research Project under grant no: 19ADP143.

**Keywords:** Amino acid, Glycine, NBO.

27

## SUA PROGRAMMING LANGUAGE'S USE IN TURKEY

**Ufuk Yıldız**

Eskişehir/Türkiye  
ufuk\_yildiz@anadolu.edu.tr

### ABSTRACT

It's organised for about national Programming Language and development to make new innovation preparing at 2014. The team's specially purpose is for take attention to beginner programmers. In this document's subtitles, I've explain to question marks.

**Keywords** : "SUA", "Programming Language", "Windows", "C#", "Turkish Command Lines"

28

## AMMONIA ADSORPTION OF NATURAL MATERIALS

**Saisha Saloni**

Mineral research institute  
India

### ABSTRACT

Ammonia nitrogen adsorption isotherm and adsorption kinetics experiments were done separately with natural zeolite, particle size 1 ~ 1.5 mm and 2 ~ 4 mm. The maximum adsorption of crude zeolite and fine zeolite to ammonia nitrogen was 5.96 (mg / g) and 17.41 (mg / g), respectively, indicating that the absorption effect of fine zeolite is better quality than that of crude zeolite. The adsorption process of natural zeolite to ammonia nitrogen was determined as a first-order reaction at a constant rate of 0.024 (g m<sup>-3</sup> h<sup>-1</sup>).

## EXAMINATION OF VANADIUM EFFECT ON GENERAL MECHANICAL CHARACTERISTICS OF BI-2223 MATERIALS VIA SEMI-EMPIRIC MODELS

Ugur SOYKAN<sup>1,\*</sup>, Fidan VELIYEVA<sup>2</sup>, Gurcan YILDIRIM<sup>3</sup>

<sup>1</sup>Yenicaga Yasar Celik Vocational High School, Bolu Abant Izzet Baysal University, Bolu-Turkey, 14300

<sup>2</sup>Department of Chemistry, Bolu Abant Izzet Baysal University, Bolu-Turkey, 14000

<sup>3</sup>Bolu Abant Izzet Baysal University, Department of Mechanical Engineering, Bolu-Turkey, 14280  
e-mail of the corresponding author: [ugursoykan@ibu.edu.tr](mailto:ugursoykan@ibu.edu.tr)

### ABSTRACT

In the current work, we semi-empirically investigate the load-independent Vickers hardness values of vanadium added Bi-2223 compounds in the plateau limit regions evaluated from the experimental microhardness graphics (Vickers hardness parameters versus applied indentation test loads) to determine the role of vanadium particles on the general mechanical characteristics with the aid of six mechanical modeling approaches, namely law of Meyer, proportional sample resistance, elastic/plastic deformation, modified proportional sample resistance, Hays-Kendall and indentation-induced cracking models. Throughout the study, the samples are prepared with the different molar rations varying from  $x=0$  to 0.3 by the conventional ceramic method in the normal atmospheric pressure at the room temperature conditions. All the model findings show that the mechanical performances tend to constantly reduce with increasing the vanadium concentration level embedded in the Bi-2223 superconducting crystal system. This is in accordance to the fact that the concentration level of vanadium remarkably damages the main structural problems and permanent irreversible deformations. In this respect, it is not wrong to verify that the vanadium inclusions unstabilize the inherit durable tetragonal phase of Bi-2223 inorganic solids, resulting in the regression in the mechanical durability (resistance towards to the applied loads) in case of the applied test loads. Moreover, the models indicate that every material prepared exhibits the conventional indentation size effect (related to the formation of elastic and plastic deformations in the host crystal structures simultaneously due to the recovery of systems) but within the suppression trend. Shortly, all the semi-empiric models preferred in the present work are found to be useful descriptors to define the suitable relationship between the ion-addition mechanism in the crystal lattice and mechanical durability/performances of vanadium-added Bi-2223 materials. We should, of course, declare here that the indentation-induced cracking approach is gathered to be the best approach model for the load-independent Vickers hardness values in the plateau limit regions.

**Keywords:** Vanadium-added Bi-2223 material; Semi-empiric models; Mechanical durability; Plateau limit regions.

## A COMPARATIVE STUDY OF CLASSIFICATION METHODS ON HUMAN SKIN DETECTION FROM RGB AND YCBCR REPRESENTED COLOR IMAGES

Utku KAYA<sup>1,\*</sup>, Murat BAŞARAN<sup>1</sup>

<sup>1</sup> Vocational School of Transportation, Eskişehir Technical University Eskişehir, Turkey

### ABSTRACT

Skin detection has an important place in image processing. Human-computer interaction has made this study area very popular. The most common color space used in skin detection is Red Green and Blue but RGB space can be converted into YCbCr space. Both features give strong information about the properties of the images. In this study, RGB and YCbCr spaces are used to detect human skin. The extracted features are trained by several classification methods. The obtained features are used to segment the human skin by using the chosen classification algorithm and finally, the promising performance results are presented comparatively with the most commonly used classifications methods in the literature.

**Keywords:** Feature extraction, Image segmentation, YCbCr

## AN EFFICIENT AND SOLVENT FREE SYNTHESIS of N-Aryl 2,3-DIHYDRO-4H NAPHTHO-[2,1-E] 1,3-OXAZINES

Mohammad S.Al-Ajely and Ahmed M Noori

Chemistry Dept.College of Education for girls,Mosul University ,Mosul-Iraq

### Abstract

Oxazine compounds have proved to have many pharmaceutical applications and most of these compounds now a days are used as drugs. For the importance of this class of heterocyclic compounds we are here investigate the synthesis of new derivatives of 1,3-oxazines using solvent free one pot three component system in a drug discovery program ,so starting from  $\beta$ -Naphthol, formaldehyde and aromatic amines in presence of zarconyl chloride as catalyst. compounds 1-9 were synthesized, Benzo 1,3 diazines(10-14) were also synthesized from their corresponding 1,3 oxazines .These compounds were characterized by IR, some representative by <sup>1</sup>HNMR and were discussed.

**Keywords;** Aryl,1,3-Naphthoxazines,Solvent free

### ADSORPTION OF SOME ANIONS BY SEPIOLITE BELONGS TO ESKISEHIR (SİVRİHİSAR) REGION AND SURFACE ACTIVE AGENTS-MODIFIED FORMS

Sedef DİKMEN

<sup>1</sup> Department of Physics, Faculty of Science, Eskisehir Technical University, Eskisehir, Turkey

#### ABSTRACT

In this research, firstly a natural clay mineral, which is sepiolite, was transformed into Na-sepiolite forms and then Na-sepiolite were modified by hexadecyltrimethylammonium (HDTMA) bromide [ $\text{CH}_3(\text{CH}_2)_{15}\text{N}(\text{CH}_3)_3\text{Br}$ ]. The characterization studies by using different methods (BET, XRF, XRD, SEM, FT-IR, TG/DTA, immersion heat and zeta potential measurement) were also carried out to identify the modification of natural sepiolite with HDTMA-Br and its adsorption behaviour. Then, the adsorption of hazardous anions, which are present in wastewater or underground water with HDTMA-sepiolite were investigated in batch technique. In this manner, the effects of adsorbent dosage, contact time and pH were investigated for the adsorption of nitrate, sulphate and phosphate anions onto HDTMA-sepiolite. Adsorption kinetics and isotherm parameters were deduced by using experimental data. Pseudo-first-order, pseudo-second-order and Weber-Morris models and Langmuir and Freundlich isotherms were applied to the experimental data to obtain adsorption kinetics and adsorption equilibrium, respectively. According to this, the adsorption of phosphate anion data fit well with the pseudo-second-order kinetic model (with high correlation coefficients).

**Keywords:** Anion adsorption, HDTMA-sepiolite, isotherm.

### A NOVEL METHOD FOR SPERM QUANTIFICATION IN THE AFRICAN MALARIA MOSQUITO ANOPHELES GAMBIAE S.L

Nkiru E Ekechukwu, Felicia N Ekeh, Chinenye M Ohanu, Greg E Odoh:

Department of Zoology and Environmental Biology, Faculty of Biological Sciences, University of Nigeria, Nsukka, Nigeria.

#### ABSTRACT

The success of vector control projects such as the Sterile Insect Technique and Release of Insects carrying a Dominant Lethal gene for malaria control relies on the mating fitness, mating competitiveness and reproductive investment trade-offs of released laboratory-reared males. Determination of these factors has proven to be difficult, particularly the reproductive investment such as sperm numbers, where the existing technique used can only provide approximations. We, therefore developed a qPCR technique based on TaqMan assay, to quantify sperm numbers in the female spermatheca after mating. Y-chromosome specific primers and probe were designed, optimized and used for the amplification of Y-chromosome in the sperm transferred by males. Genomic DNA was extracted from adult males and used to generate serial dilution for a standard curve. A best-fit log-quadratic equation generated from the standard curve was used to translate the cycle threshold values of individual sperm samples into sperm number. The repeatability of the technique was tested on stored and fresh sperm bundles from field-collected and lab-reared females. A positive correlation was observed between repeated measures of the same sample, suggesting that the technique could be a successful ecological tool to determine reproductive investments in insects for vector control purposes while highlighting the importance of male reproductive investments in *Anopheles gambiae s.l* which presently is lacking.

**Keywords:** *An. coluzzii*, *An. gambiae s.s.*, sperm quantification, Taqman qPCR assay, sperm numbers



## SEMI SYMMETRICAL MOLECULES' SYMMETRY AND REFLECTION OPERATIONS WITH CLIFFORD ALGEBRA

Abidin Kılıç<sup>1</sup> Mine Fakılı<sup>2</sup>

<sup>1</sup> Department of Physics, Faculty of Science, Eskisehir Technical University, Eskisehir, Turkey  
<sup>2</sup> Graduate Education Institute, Eskisehir Technical University, Eskisehir, Turkey

### ABSTRACT

The Clifford algebra produces the new fields of view in the molecular and mathematical physics, definition of bodies and rearranging for equations of mathematics and physics. The new mathematical models play an important role in the progress of physics. After presenting Clifford algebra and quaternions, the symmetry operations in molecular physics with Clifford algebra and quaternions are defined. This symmetry operations are applied to some symmetric and semi-symmetric solids too. Also, the vertices of some symmetric semisymmetric solids presented in the Cartesian coordinates are calculated.

## SPECTRAL MONITORING OF THE HERBIG AE STAR HD 179218

*Adigozalzade H.N.*

N.Tusi Shamakhy Astrophysical Observatory of Azerbaijan National Academy of Sciences  
ismailovnshao@gmail.com

### ABSTRACT

Spectral observations of the star were performed at the Cassegrain focus of the 2 m Karl Zayss telescope of ShAO of Azerbaijan NAS by using an echelle spectrometer constructed on the base of the spectrograph UAGS. As a light detector we have used a CCD with 530x580 elements. Observations were performed in the range  $\lambda$  4700-6700 Å. The spectral resolution is  $R = 14000$ . The mean signal to noise level in the region of the line  $H\alpha$  is  $S/N = 80-100$ , and in the region of the line  $H\beta$ , is  $S/N = 30-40$ . Reduction and calibration of the spectrograms is performed in the DECH programs. We are present results monitoring of the spectral variability of the star on spectral lines obtained in the visual range of spectrum.

EUTECTIC PHASE CRYSTALLIZATION IN  $\text{Co}_{0,55}\text{Sb}_{0,45}\text{-Sn}$  and  $\text{Co}_3\text{Sn}_2\text{-Sb}$  SYSTEMSSayyara SADIQOVA<sup>1,\*</sup>, Mahmud ALLAZOV<sup>2</sup>, Chingiz ABILOV<sup>1</sup><sup>1</sup> Electronics, Electric Power Engineering and Automatics, Azerbaijan Technical University, Baku, Azerbaijan<sup>2</sup> Industrial Ecology and Safety of Life Activity, Metallurgical and Materials Engineering, Azerbaijan Technical University, Baku, Azerbaijan

## ABSTRACT

Eutectic compositions crystallized under ordinary conditions have high thermal stability. There is no chemical interaction between the eutectic and the phases forming it. This allows them to be used as antidiffusion layers in the contact between a conductor and a semiconductor. We have established that solders based on eutectic compositions of the ternary Ni-Sn-Bi system have high strength mechanical characteristics [1]. The binary phases of the ternary Co-Sn-Sb system also have valuable applied properties. In particular, CoSb-based phases have superconductivity,  $\text{Co}_3\text{Sn}_2$  has a sufficiently high microhardness, etc. [2]. Therefore, interest in the study of the ternary Co-Sn-Sb system is due to the manufacturing of eutectic composition materials with improved electrophysical, as well as with high-strength mechanical properties.

Synthesis of  $\text{Co}_{0,55}\text{Sb}_{0,45}\text{-Sn}$  system alloys was performed by ampoule method [3] by joint fusion of especially pure cobalt elements, tin and antimony at 1000 °C, followed by slow cooling at a rate of  $\sim(10-15)$  deg/min. Alloys in the solid state were heat treated. Studies of the alloys brought to equilibrium were carried out by differential thermal, X-ray phase and microstructural analyzes with microhardness and pycnometric density measurements.

A phase diagram of the intersecting  $\text{Co}_{0,55}\text{Sb}_{0,45}\text{-Sn}$  and  $\text{Co}_3\text{Sn}_2\text{-Sb}$  sections is constructed. It is established that the first section is quasibinary and its phase diagram represents an eutectic character. The eutectic of this section is degenerate near the tin component and has a crystallization temperature of 231 °C.

The interaction of components in the  $\text{Co}_3\text{Sn}_2\text{-Sb}$  section is more complex. Up to the point of intersection (63 mol% Sb) in the subsolidus of the system at first crystallize CoSb,  $\text{Co}_3\text{Sn}_2$  and Sn, and then the phases of CoSb, Sb, and Sn.

**Keywords:** eutectic compositions, phase crystallization, phase diagram

## REFERENCES

- [1] Sadiqova S.G., Allazov M.R., Abilov Ch.I. Phase equilibrium in  $\text{Ni}_3\text{Sn-Bi}$  system // Scientific works of Azerbaijan Technical University (AzTU), Fundamental Sciences. Baku, AzTU Publishing House, 2010, VII (26): 28-29.
- [2] Samsonov G.V., Abdusalyamova M.N. Antimonides. Dushanbe, Donish Publishing House, 1977; 246 p.
- [3] Andreev O.V. Synthesis of intermetallic semiconductor and superconducting materials. // Tyumen, Tyumen State University Publishing House, 1990, p. 114

**THE BIFUNCTIONAL CATALYST Pt / Re USED IN THE PLATFORMING UNIT FOR OBTAINING HIGH OCTANE NUMBER OF THE GASOLINE.**

Menouar HANAFI

The University of Science and Technology of Oran, ALGERIA

Faculty of Chemistry

E-Mail: [hanafi951@yahoo.com](mailto:hanafi951@yahoo.com)

**ABSTRACT**

The original function of the process of platforming is to develop heavy naphtha (HSRN), coming from the atmospheric unit of distillation with a weak octane number (NO = 44), to obtain a mixture of fuels whose octane number is raised by catalytically supporting specific groups of chemical reactions. The installation is divided into two sections:

□□□ Section hydrobon. Section platforming.

The raffinate coming from the bottom of column 12C2 to feed the section platforming, is divided into two parts whose flows are controlled and mixed with gas rich in hydrogen.

Bottom of the column, one obtains stabilized reformat which is aspirated by their pump to ensure the heating of the column whereas a part is sent towards storage after being cooled by the air cooler and the condenser.

In catalytic catalyst of reforming, there is voluntarily associated a hydrogenating function - dehydrogenating, brought by platinum deposited, with an acid function brought by the alumina support (Al<sub>2</sub>O<sub>3</sub>). The mechanism of action of this bifunctional catalyst depends on the severity of the operation, of the quality of the load and the type of catalyst.

The catalyst used in the catalytic process of reforming is a very elaborate bifunctional catalyst whose performances are constantly improved thanks to the experimental research supported on an increasingly large comprehension of the phenomena.

The American company Universal Oil petroleum (UOP) marketed several series of bimetallic catalysts such as R16, R20, R30 and R62 consisted of Platinum / Rhenium on an acid support consisting of the alumina added with a halogenous compound (chlorine).

**Keywords:** Platforming, Amelioration, Octane Number, Catalyst.

**ESTIMATION OF MEL-FREQUENCY CEPSTRAL COEFFICIENTS USING PHASE INFORMATION OF VOICE SIGNAL OF AUTHENTICATION SYSTEM USER****Mykola PASTUSHENKO<sup>1,\*</sup>, Yana KRASNOZHENIUK<sup>2</sup>**

<sup>1</sup> V.V. Popovskyy Department of Infocommunication Engineering, Faculty of Infocommunications, Kharkiv National University of Radio Electronics, Kharkiv, Ukraine

<sup>2</sup> V.V. Popovskyy Department of Infocommunication Engineering, Faculty of Infocommunications, Kharkiv National University of Radio Electronics, Kharkiv, Ukraine

**ABSTRACT**

The article considers the issues of increasing the reliability of storing various resources, access to which is carried out using telecommunication networks. The first barrier in ensuring the reliability of access is the user authentication system. The preference has been recently given to access systems based on biometric user characteristics. Initially, preference was given to the static biometric characteristics of the user (face image, finger papillary pattern and the iris of the eye), which did not meet the expectations of developers and users due to the simplicity of their counterfeiting. Nowadays, dynamic (behavioral) biometric features of users, namely, voice authentication systems are more preferable. As it is known, voice authentication systems have a number of advantages: simplicity, compactness, low cost, and a number of others. In addition, the passphrase can be rapidly changed and increased during the authentication process. However, the quality indicators of all biometric access systems do not meet the increasing requirements. In the process of voice authentication, the amplitude-frequency spectrum of registration materials is analyzed. The main research is focused on the use of formant estimates, cepstrum coefficients, mel-frequency cepstral coefficients, linear prediction coefficients as a user template; and based on them, solutions are formed on the basis of the Gaussian Mixture Model and Support Vector Machine as well as Hidden Markov Models or artificial neural networks. In the report, the analysis of the amplitude-frequency spectrum is proposed to be supplemented with studies of phase data, which are traditionally ignored in this authentication. The article presents the results of studies on the estimation of mel-frequency cepstral coefficients based on the amplitude and phase information of the voice signal. The research performed has shown a high equivalence of the formed coefficients, which emphasizes the importance of the phase information of the voice signal. The results of studying the user signal when calculating mel-frequency cepstral coefficients using the amplitude and phase information are presented. It is shown that the results of calculations of mel-frequency cepstral coefficients using the phase information coincide with data obtained using the amplitude information. The latter confirms the efficiency of using phase information in the user voice authentication process.

**Keywords:** Authentication; voice signal; amplitude and phase information; cepstrum coefficients

**REFERENCES**

- [1] Beigi H. Fundamentals of Speaker Recognition. NY: Springer, 2011, 1029.
- [2] Пастушенко НС, Педро ВГ, Файзулаева ОН. Исследование информативности фазовых данных голосового сигнала пользователя системы аутентификации. In: Проблеми телекомунікацій, 2018, № 1 (22), 67–74.
- [3] Сорокин ВН, Вьюгин ВВ, Тананыкин АА. Распознавание личности по голосу: аналитический обзор. In: Информационные процессы. Moscow, РАН, 2012, Vol. 12, № 1, 1–30.
- [4] Oppenheim AV, Lim JS. The Importance of Phase in Signals: In: Proceeding of the IEEE, 1981, Vol. 69(5), 529 - 541.

**THE EFFECT OF MICROWAVE RADIATION OF LOW INTENSITY ON RED BLOOD CELLS AT ISCHEMIC STROKE****Liliya BATYUK<sup>1</sup>, Dmitry Astapovich<sup>2</sup>, Vladimir BEREST<sup>2</sup>, Natalya KIZILOVA<sup>2</sup>,  
Yury SHCKORBATOV**<sup>1</sup>Department of Medical and Biological Physics and Medical Information Science, Kharkiv National Medical University, Kharkiv, Ukraine<sup>2</sup>Department of Molecular and Medical biophysics, V. N. Karazin Kharkiv National University, Kharkiv, Ukraine**ABSTRACT**

The development of mobile communication, radar, as well as other information and energy transmission systems leads to an increase in the total level of electromagnetic radiation of different frequency ranges, intensity and modes of generation in the environment [1]. The frequency applied in the present work (36.64 GHz) belongs to the *Ka* band (27–40 GHz) used in different radar systems [2]. The study involved 10 patients aged 38-40 years who underwent ischemic stroke. The control group consisted of 10 healthy donors of the same age. The aqueous suspensions of RBCs have been exposed in EMF with frequency 36.64 GHz, the power density was 1 W/m<sup>2</sup>, exposure – 30 sec and their complex dielectric permittivity have been estimated by ultra-high frequency dielectrometry with frequency 9.2 GHz [2]. Statistical processing of the measured data was performed using the methods of variation statistics. The investigation of the cells after exposed to microwave radiation does to increase the effect changes in the viscosity of the plasma membrane and, as a consequence, indicate a change in the amount of free-bound water in the cells and the ability of cells to adequately respond to stress.

**Keywords:** microwave radiation, red blood cell, permittivity

**REFERENCES**

- [1] Batyuk L, Shckorbatov Y, Kizilova N, Astapovich D, Berest V. Study of the influence of the electromagnetic field on the state of erythrocytes of patients with acute ischemic stroke by the method of UHF dielectrometry. 3rd International Turkish Congress on Molecular Spectroscopy. Book of Abstracts 2017: 182-183.
- [2] Shckorbatov Y. The main approaches of studying the mechanisms of action of artificial electromagnetic fields on cell. J Electrical Electronic Syst 2014; 3(2): 2-8.

## INVESTIGATION OF THE QOE-AWARE ADAPTIVE MULTIPATH ROUTING MODEL WITH ASSURANCE OF THE R-FACTOR

Oleksandr LEMESHKO, Maryna YEVDOKYMENKO, Oleksandra YEREMENKO

V.V. Popovskyy Department of Infocommunication Engineering, Faculty of Infocommunications,  
Kharkiv National University of Radio Electronics, Kharkiv, Ukraine  
corresponding author: maryna.yevdokymenko@iee.org

### ABSTRACT

In this paper, the main attention is paid to solving the problem of ensuring the required QoE level using the R-factor when transmitting VoIP traffic. Based on this, the QoE-aware adaptive multipath routing model with assurance of the R-factor was developed. Within the framework of this model, the conditions of the flow conservation, the condition for preventing network congestion were introduced, and possible packet losses caused by the congestion of network elements were taken into account. A feature of the proposed model is the tensor formalization of the network, which was presented in the basis of interpolating paths and internal node pairs. As a main result, thanks to this tensor representation of the network, improved expressions were obtained in an analytical form for calculating the indicators of the average end-to-end delay and the probability of packet loss. The obtained expressions according to the recommendations of ITU-T G.109 and G.107 were used to assess the QoE level by the R-factor.

As an optimality criterion, the minimum of a linear function was chosen, which is focused on ensuring a more balanced use of the network resource depending on the values of the routing variables and metrics of communication links. The study of the proposed adaptive routing model was carried out on a fragment of the telecommunication network, in which the requirements for the QoE level were set by the R-factor. As a result of calculations, the values of the average end-to-end delay, the probability of packet loss, and subsequently the R-factor were obtained, the values of which coincided with the required ones. Particular attention should be paid to the fact that with an increasing the requirements for the QoE level by the R-factor, the volume of the used network resource gradually increased, new routes were used from the node-source to the node-receiver.

**Keywords:** quality of experience; average end-to-end delay; packet loss; R-factor; telecommunication network

41

## THE DARK MATTER AND ENERGY IN THE DE SITTER WORLD

Bala Ali RAJAVOV

N.Tusi Shamakhi Astrophysics Observatory, National Academy of Sciences of Azerbaijan, Baku,  
Azerbaijan

### ABSTRACT

It is shown that dark matter and energy are cosmological quantum effects. De Sitter's world is considered as a cosmological model. It is shown that in the de Sitter world, gravity and antigravity are different states of the elementary quantum Wigner's system. In the limiting case of the Minkowski world, antigravity can be excluded. Moreover, it is shown that the Wigner - Inönü limit of the de Sitter model to the Minkowski world plays the role of Bohr's correspondence principle in quantum mechanics.

**Keywords:** de Sitter world, Wigner-Inönü limit, "dark" matter and energy, Wigner's elementary systems, correspondence principle

### REFERENCES

[1] Rajabov B.A., The contraction of the representations of the group SO 4,1 and cosmological interpretation, *Astronomy&Astrophysics (Caucasus)*, 2018; 3: 74-90.

42

## MATHEMATICAL MODEL OF THE DEVELOPMENT OF MANUFACTURING DEFECTS IN THE SURFACE LAYER OF SUBSTRATES OF MOEMS' FUNCTIONAL COMPONENTS

Igor NEVLIUDOV<sup>1</sup>, Murad OMAROV<sup>2</sup>, Olena CHALA<sup>1</sup>

<sup>1</sup> Department of Computer-Integrated Technologies, Automation and Mechatronics, Kharkiv National University of Radio Electronics, Kharkiv, Ukraine

<sup>2</sup> Faculty of Automatics and Computerized Technologies, Kharkiv National University of Radio Electronics, Kharkiv, Ukraine

### ABSTRACT

A mathematical model of the development of manufacturing defects, with the prediction of the random component of the model in the substrates of functional components of MOEMS, which are made of semiconductors, in particular, silicon, are developed in the article.

The main manufacturing defects that arise in the surface layer of the substrates of the MOEMS functional components taking into account the technological processes of their production and dynamic processes were used when developing the model.

The developed mathematical model takes into account the occurrence of a random component of the model with its predictive ability.

The possibility of such control is the basis for the development of the scientific direction of technology and equipment for the production of semiconductors, materials and electronic devices - defect engineering, based on the management and forecasting of defect formation processes.

**Keywords:** mathematical model, defect, MOEMS, functional components.

ISBN: 978-605-69034-6-5

# **ICONAT 2020**

**BAKU-AZERBAIJAN**

**AUGUST 20-22, 2020**

## **FULL TEXTS**



## NATURAL BOND ORBITAL INTERACTION ANALYSIS OF GLYCINE

Saliha ILICAN, Nihal KUŞ

Department of Physics, Science Faculty, Eskisehir Technical University, Yunus Emre Campus, 26470 Eskisehir, Turkey

### Abstract

In this study, the glycine (*Gly*; C<sub>2</sub>H<sub>5</sub>NO<sub>2</sub>) molecule was theoretically analyzed using natural bond orbital (NBO) interactions with density functional theory (DFT)/B3LYP/6-311++G(d, p) method. All calculations were performed for three main conformers with minimum energy state. Donor-acceptor interactions of *Gly* were calculated using second order Fock matrix Schrödinger equation. Effects of bond polarization and hybridization were analyzed in wave functions associated with the formation of conformers. The global reactivity descriptors such as electronegativity ( $\chi$ ), electronic potential ( $\mu$ ), hardness ( $\eta$ ), softness ( $\sigma$ ) and global electrophilicity index ( $\omega$ ) were calculated for three main conformers of *Gly*. The molecular electrostatic potential (MEP) energy surfaces of the molecule allow us to identify charged regions that vary in a molecule. MEP surfaces were plotted for three main conformers of *Gly* molecule calculated by density functional theory with B3LYP/6-311++G(d, p) level.

**Keywords:** Amino Acid, Glycine, NBO, Stabilization energy.

### 1. INTRODUCTION

Amino acids are organic molecules having biological significance. There are more than seven hundred amino acids in nature. About 20 of these amino acids are encoded by DNA. These also form proteins. The reason why there is a different type of protein in every living being is that the number, type and sequence of amino acids are different from each other (E-Dalatony et al., 2019; Michalski and Januel; 2006; Wagner and Musso, 1983). It is therefore of great importance to know the structure of amino acids, which are directly related to the structure of living beings.

Glycine (*Gly*; IUPAC: 2-aminoacetic acid; C<sub>2</sub>H<sub>5</sub>NO<sub>2</sub>), one of these amino acids, is structurally the simplest. *Gly* is used in the biosynthesis process of proteins. It is a non-essential amino acid, and can be synthesized by the body. In order to make considerable compounds, such as glutathione, creatine and collagen, the body requires *Gly*. On the other hands, it is also used in some treating such as protect liver from alcohol-induced damage, improve sleep quality and heart health. But perhaps most important is its use in cancer prevention and memory development.

There are both theoretical and experimental studies regarding *Gly* in the literature (Kuş and Ilican, 2019; Coussan and Tarczay, 2016; Bzásó, et al., 2012; Selvarengan and Kolandaivel, 2004; Kieninger et al., 1998, Stepanian et al., 1998; Reva et al., 1995). In our previous study (Kuş and

Ilican, 2019), we studied the conformations of *Gly* molecule with the using DFT with B3LYP/6-311++G(d,p) basis set, and determined that there are seven conformers and three of them are the main conformers. In the present study, Natural Bond Orbital (NBO) calculations for the three main conformers of *Gly* were made and analyzed.

## 2. THEORITICAL DETAILS

The calculations were performed with the Gaussian09 (Frisch et al., 2009) program. Stabilization energies and orbital analysis of the *Gly* were clarified using the NBO theory. The method was used considering Weinhold and co-workers, by NBO 3.1 (Reed et al, 1988) as integrated in Gaussian 09. The global reactivity descriptors were calculated with B3LYP/6-311++G(d,p) level (Becke, 1988; Lee et al., 1988).

## 3. RESULTS AND DISCUSSION

In our previous study (Kuş and Ilican, 2019), *Gly* molecule was optimized using DFT with B3LYP/6-311++G(d,p) basis set and found seven conformers with minimum energy. But three of them are main conformers (Fig. 1). Owing to the calculations, *GlyI* is more stable than *GlyII* and *GlyIII* conformers, respectively. The electronic energy differences ( $\Delta E$ ) between *GlyI* and *GlyII*, *GlyI* and *GlyIII* are 1.78 and 6.37 kJ mol<sup>-1</sup>, respectively.

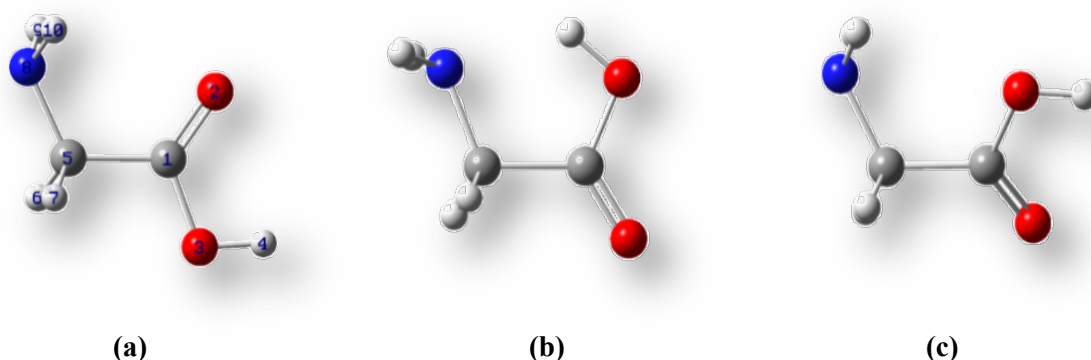


**Figure 1.** The molecular structure of three main conformers for *GlyI*, *GlyII* and *GlyIII*, calculated by B3LYP/6-311++G(d,p) level.

The orbital energies for selected NBO pairs of three main conformers for *GlyI*, *GlyII* and *GlyIII* were calculated using the Fock matrix equation, and given in the Table 1.  $E(2)$  stabilization energies, between donor (filled) and acceptor (empty) NBOs, were estimated by the second-order perturbation approach (Weinhold and Landis, 2005),

$$E(2) = \Delta E_{ij} = q_i \frac{F_{ij}^2}{\varepsilon_j - \varepsilon_i} \quad (1)$$

where  $q_i$  is the donor orbital occupancy,  $\varepsilon_i$  and  $\varepsilon_j$  are the diagonal elements and  $F_{ij}$  is NBO the off-diagonal NBO Fock matrix element. In the calculations, the difference in acceptor and donor energy was taken into account together with  $q_i$  donor orbital occupation ( $\varepsilon_j - \varepsilon_i$ ). As can be seen from Table 1, it has been found that the highest stabilization energy for the three main conformations is at

LP2(O3)  $\rightarrow$   $\pi^*(\text{C1-O2})$  transitions (*ca.*183 kJ mol<sup>-1</sup> for *GlyI*, *ca.*184 kJ mol<sup>-1</sup> for *GlyII*, *ca.*183 kJ mol<sup>-1</sup> for *GlyIII*). The lowest one is at LP1(N8)  $\rightarrow$   $\sigma^*(\text{C1-C5})$  transitions for *GlyI* (*ca.*37 kJ mol<sup>-1</sup>) and *GlyIII* (*ca.*42 kJ mol<sup>-1</sup>), and LP1(N8)  $\rightarrow$   $\sigma^*(\text{O3-H4})$  transition for *GlyII* (*ca.*44 kJ mol<sup>-1</sup>).

**Table 1.** Donor and acceptor pairs, orbital energies for selected NBO pairs as calculated by the Fock matrix equation (Eq.1) in the NBO basis for three main conformers of *Gly*<sup>a</sup>.

| <i>Conformer</i> | <i>Donor NBO</i> | <i>Acceptor NBO</i>      | <i>E(2)</i>          | $\epsilon_j - \epsilon_i$ | <i>F<sub>ij</sub></i> |
|------------------|------------------|--------------------------|----------------------|---------------------------|-----------------------|
|                  | (i)              | (j)                      | kJ mol <sup>-1</sup> | au                        | au                    |
| <i>GlyI</i>      | LP1(O2)          | Ry1*(C1)                 | 72.98                | 1.67                      | 0.152                 |
|                  | LP2(O2)          | $\sigma^*(\text{C1-O3})$ | 139.82               | 0.61                      | 0.130                 |
|                  | LP2(O2)          | $\sigma^*(\text{C1-C5})$ | 77.29                | 0.64                      | 0.099                 |
|                  | LP2(O3)          | $\pi^*(\text{C1-O2})$    | 182.88               | 0.35                      | 0.111                 |
|                  | LP1(N8)          | $\sigma^*(\text{C1-C5})$ | 37.12                | 0.67                      | 0.069                 |
| <i>GlyII</i>     | LP1(O2)          | Ry1*(C1)                 | 70.43                | 1.74                      | 0.153                 |
|                  | LP2(O2)          | $\sigma^*(\text{C1-O3})$ | 131.46               | 0.63                      | 0.128                 |
|                  | LP2(O2)          | $\sigma^*(\text{C1-C5})$ | 82.39                | 0.60                      | 0.099                 |
|                  | LP2(O3)          | $\pi^*(\text{C1-O2})$    | 184.05               | 0.36                      | 0.113                 |
|                  | LP1(N8)          | $\sigma^*(\text{O3-H4})$ | 43.60                | 0.74                      | 0.079                 |
| <i>GlyIII</i>    | LP1(O2)          | Ry1*(C1)                 | 70.98                | 1.67                      | 0.150                 |
|                  | LP2(O2)          | $\sigma^*(\text{C1-O3})$ | 142.04               | 0.61                      | 0.130                 |
|                  | LP2(O2)          | $\sigma^*(\text{C1-C5})$ | 73.86                | 0.63                      | 0.096                 |
|                  | LP2(O3)          | $\pi^*(\text{C1-O2})$    | 182.75               | 0.35                      | 0.112                 |
|                  | LP1(N8)          | $\sigma^*(\text{C1-C5})$ | 42.26                | 0.67                      | 0.074                 |

<sup>a</sup> See atom numbering in Fig. 1. LP: lone-pair orbital, Ry: Rydberg orbital.

NBO interactions of three main conformers are plotted also in Figures 2-4.

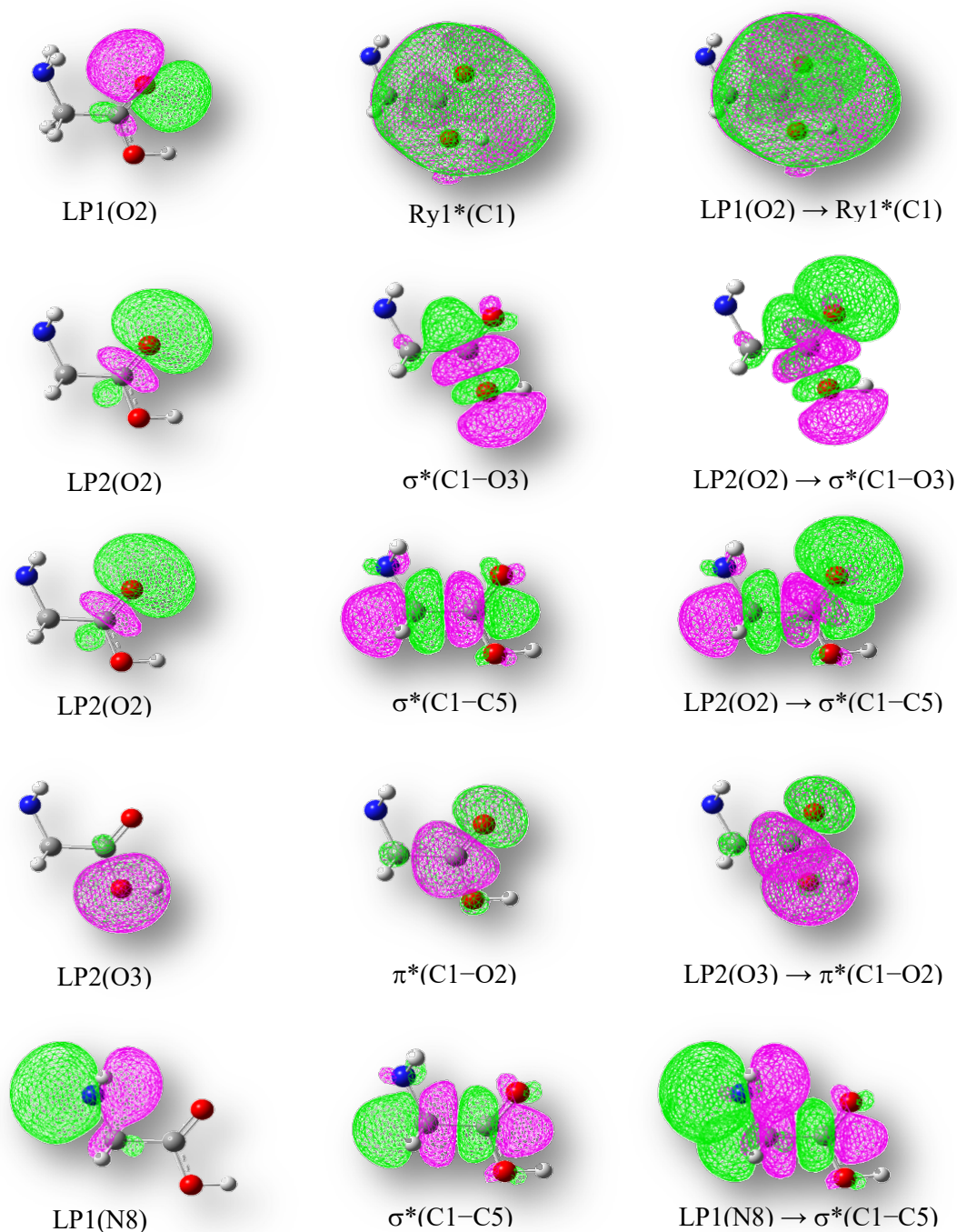


**Figure 2.** Electron density surfaces of selected NBOs for *GlyI* calculated at the B3LYP/6-311++G(d,p) level of theory showing the dominant orbital interactions (see Table 1). Isovalues of the electron densities are equal to 0.02e. Green and fuchsia colors indicate the states of positive and negative wave functions, respectively.

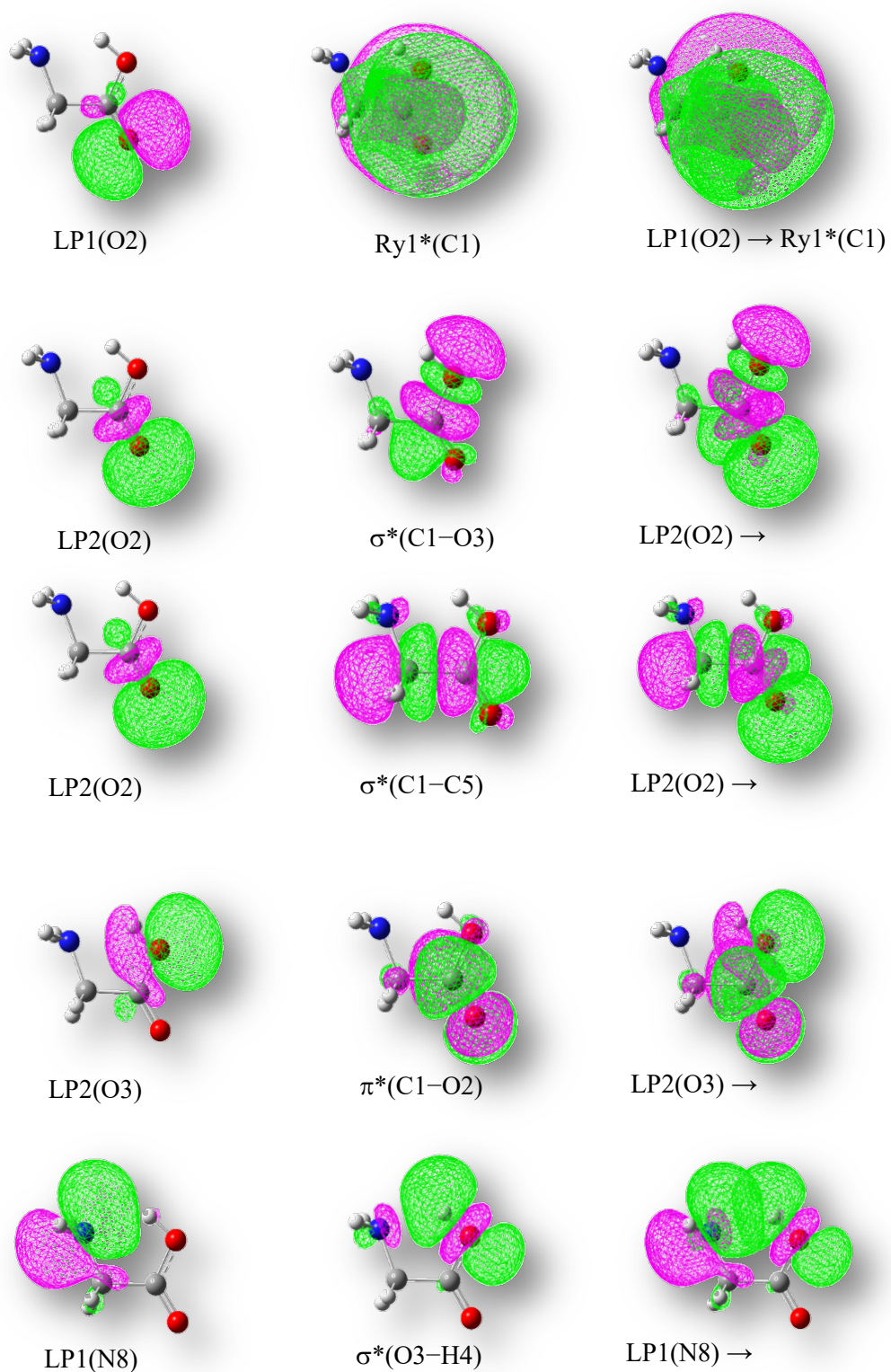


**Figure 3.** Electron density surfaces of selected NBOs for *GlyII* calculated at the B3LYP/6-311++G(d,p) level of theory showing the dominant orbital interactions (see Table 1). Isovalues of the electron densities are equal to 0.02e. Green and fuchsia colors indicate the states of positive and negative wave functions, respectively.

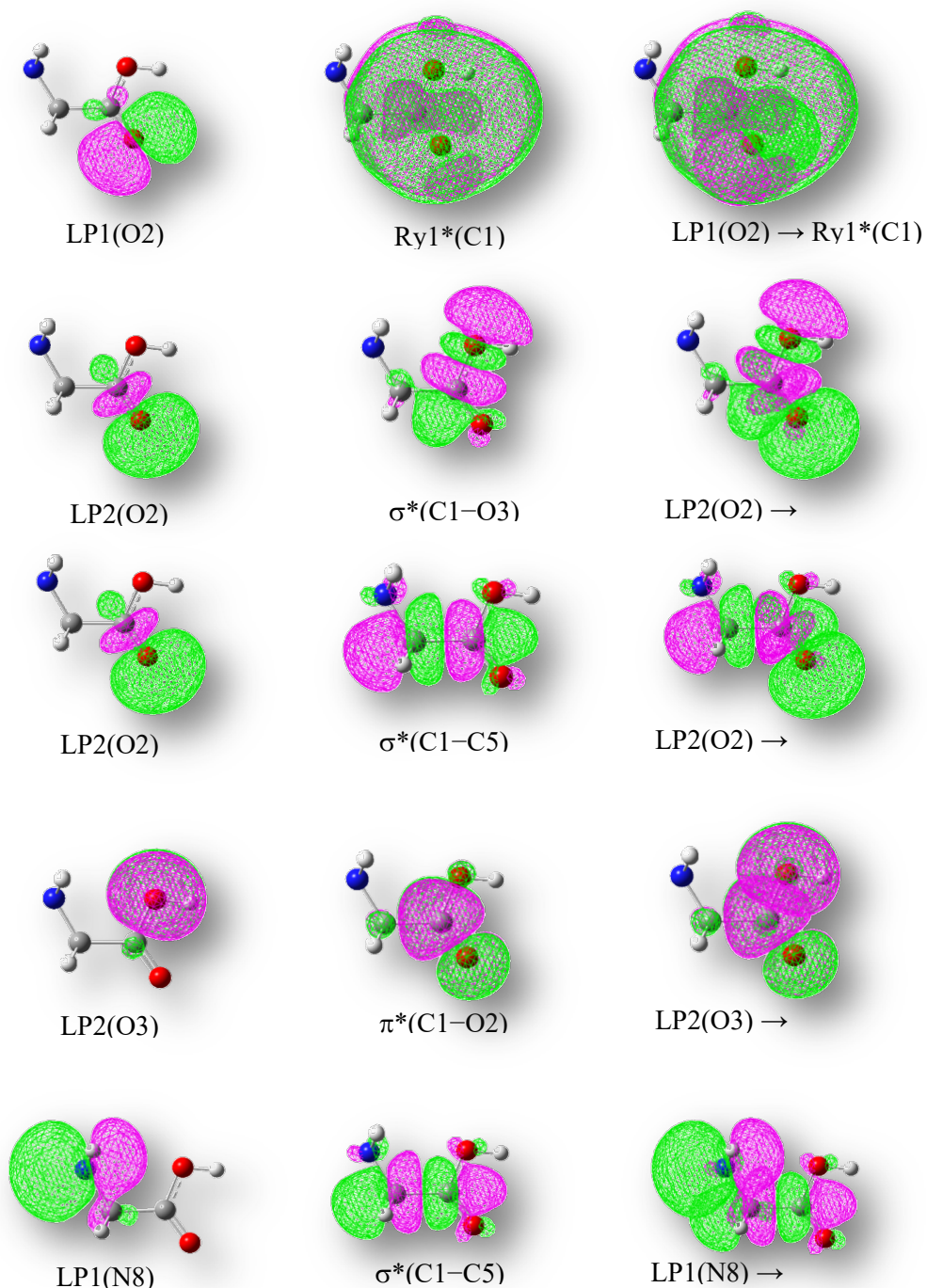


**Figure 4.** Electron density surfaces of selected NBOs for *GlyIII* calculated at the B3LYP/6-311++G(d,p) level of theory showing the dominant orbital interactions (see Table 1). Isovalues of the electron densities are equal to 0.02e. Green and fuchsia colors indicate the states of positive and negative wave functions, respectively.

Mapping of molecular electrostatic potential (MEP) surfaces of the three main conformers of *Gly* were carried out with GaussView 5 visualization program, and these surfaces are given in Fig. 5. In order to better understand the charge regions of these conformers are visualized by these maps. The red and blue colours indicate negative and positive values, respectively. The maps of *Gly* main conformers showed that the positive potentials are most concentrated around the N8 atom and O-H bonds while the negative potentials are most concentrated on C=O bound.

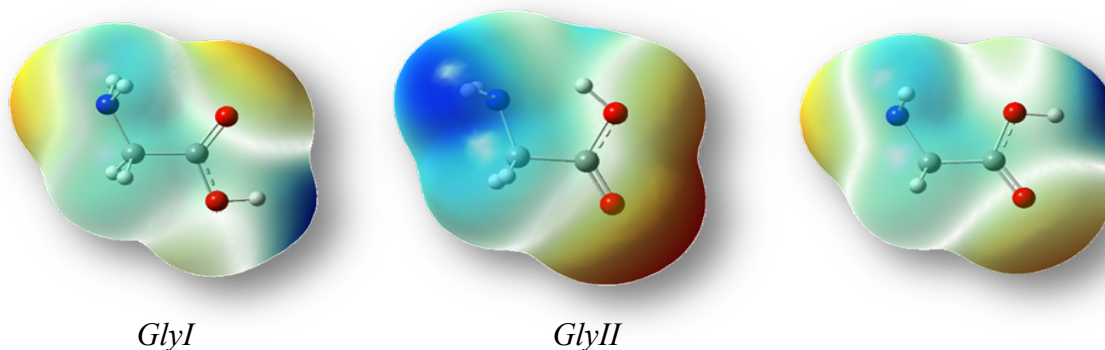


**Figure 5.** Molecular electrostatic potential (MEP) surfaces of main three *Gly* conformers, calculated with DFT/B3LYP/6-311++G(d,p) method.

In the closed-shell Hartree-Fock theory, Koopmans' theorem (Koopmans, 1934) allows the ionization potential ( $IP$ ) and electron affinity ( $EA$ ), and these values are given in following equations:

$$IP = -E_{HOMO} \quad (2)$$

$$EA = -E_{LUMO} \quad (3)$$

where  $E_{HOMO}$  is the highest occupied molecular orbital energy and  $E_{LUMO}$  is the lowest unoccupied molecular orbital energy. There is no official proof of this theorem in DFT, but the theorem is generally considered valid.

In order to understand global stability and chemical reactivity of the *Gly* molecule, we have investigated the frontier molecular orbitals (FMOs). The global reactivity descriptors such as, The  $IP$ ,  $EA$ , electronegativity ( $\chi$ ), electronic potential ( $\mu$ ), hardness ( $\eta$ ), softness ( $\sigma$ ) and global electrophilicity index ( $\omega$ ) were calculated with B3LYP/6-311++G(d,p) level using the following equations:

$$\chi = -\frac{(E_{LUMO} + E_{HOMO})}{2} \quad (4)$$

$$\mu = \frac{(E_{LUMO} + E_{HOMO})}{2} \quad (5)$$

$$\eta = \frac{(E_{LUMO} - E_{HOMO})}{2} \quad (6)$$

$$\sigma = \frac{2}{(E_{LUMO} - E_{HOMO})} \quad (7)$$

$$\omega = \frac{(E_{LUMO} + E_{HOMO})^2}{4(E_{LUMO} - E_{HOMO})} \quad (8)$$

The results are summarized in Table 2.

**Table 2.** *IP*, *EA*,  $\chi$ ,  $\mu$ ,  $\eta$ ,  $\sigma$ ,  $\omega$  and  $\Delta E_{HOMO-LUMO}$  of the main conformers of *Gly* calculated at the B3LYP/6-311++G(d,p) level of theory.

| <i>Conformer</i> | <i>IP</i> (eV) | <i>EA</i> (eV) | $\chi$ (eV) | $\mu$ (eV) | $\eta$ (eV) | $\sigma$ (eV <sup>-1</sup> ) | $\omega$ (eV) | $\Delta E_{HOMO-LUMO}$ (eV) |
|------------------|----------------|----------------|-------------|------------|-------------|------------------------------|---------------|-----------------------------|
| <i>GlyI</i>      | 7.165          | 0.471          | 3.818       | -3.818     | 3.347       | 0.299                        | 2.178         | 6.695                       |
| <i>GlyII</i>     | 7.388          | 0.916          | 4.152       | -4.152     | 3.236       | 0.309                        | 2.664         | 6.472                       |
| <i>GlyIII</i>    | 6.963          | 0.587          | 3.775       | -3.775     | 3.188       | 0.314                        | 2.236         | 6.376                       |

#### 4. CONCLUSIONS

The stabilization energies and orbital interactions of the three main conformers of *Gly* were determined using the NBO method. Electron density surfaces of selected NBOs for *Gly* calculated at the B3LYP/6-311++G(d,p) level and plotted for showing the dominant orbital interactions. The global reactivity descriptors (such as, ionization potential, electron affinity, electronegativity, electronic potential, hardness, softness and global electrophilicity index were calculated using B3LYP/6-311++G(d,p) level. MEP surface of *Gly* was plotted and analysed.

#### ACKNOWLEDGEMENT

This work was supported by Eskisehir Technical University Commission of Research Project under Grant no. 19ADP143.

#### REFERENCES

- Bazsó, G., Magyarfalvi, G. Tarczay, G. (2012). Near-infrared laser induced conformational change and UV laser photolysis of glycine in low-temperature matrices: Observation of a short-lived conformer. *J. Mol. Struct.* 1025, 33–42.
- Becke, A.D. (1988). Density-functional exchange-energy approximation with correct asymptotic behavior. *Phys. Rev. A* 38, 3098–3100.
- Coussan, S., Tarczay, G. (2016). Infrared laser induced conformational and structural changes of glycine and glycine-water complex in low-temperature matrices. *Chem. Phys. Lett.* 644, 189–194.
- E-Dalatony, M.M., Saha, S., Govindwar, S.P., A-Shanab, R.A.I., Jeon, B.H. (2019). Biological Conversion of Amino Acids to Higher Alcohols. *Trends Biotechnol.* 37, 855–869.



Frisch, M.J., Trucks, G.W., Schlegel, H.B., Scuseria, G.E., Robb, M.A., Cheeseman, J.R., Scalmani, G., Barone, V., Mennucci, B., Petersson, G.A., Nakatsuji, H., Caricato, M., Li, X., Hratchian, H.P., Izmaylov, A.F., Bloino, J., Zheng, G., Sonnenberg, J.L., Hada, M., Ehara, M., Toyota, K., Fukuda, R., Hasegawa, J., Ishida, M., Nakajima, T., Honda, Y., Kitao, O., Nakai, H., Vreven, T., Montgomery, J.A., Peralta, Jr. J.E., Ogliaro, F., Bearpark, M., Heyd, J.J., Brothers, E., Kudin, K.N., Staroverov, V.N., Kobayashi, R., Normand, J., Raghavachari, K., Rendell, A., Burant, J.C., Iyengar, S.S., Tomasi, J., Cossi, M., Rega, N., Millam, J.M., Klene, M., Knox, J.E., Cross, J.B., Bakken, V., Adamo, C., Jaramillo, J., Gompert, R., Stratmann, R.E., Yazyev, O., Austin, A.J., Cammi, R., Pomelli, C., Ochterski, J.W., Martin, R.L., Morokuma, K., Zakrzewski, V.G., Voth, G.A., Salvador, P., Dannenberg, J.J., Dapprich, S., Daniels, A.D., Farkas, O., Foresman, J.B., Ortiz, J.V., Cioslowski, J., Fox, D.J. (2009). Gaussian 09, Revision A.0.2, Gaussian, Inc., (Wallingford CT).

Kieninger, M., Suhai, S. Ventura, O.N. (1998). Glycine conformations: gradient-corrected DFT-studies. *J. Mol. Struct. Theochem.* 433, 193–201.

Koopmans, T. (1934). Über die Zuordnung von Wellenfunktionen und Eigenwerten zu den Einzelnen Elektronen Eines Atoms. *Physica* 1, 104–113.

Kuş, N., Ilican, S. (2019). Conformational and Infrared Spectrum Analysis of Glycine. *Proceeding Book of 6<sup>th</sup> International Conference on Materials Science and Nanotechnology For Next Generation*, 310-314.

Lee, C., Yang, W., Parr, R.G. (1988). Development of the Colle-Salvetti correlation-energy formula into a functional of the electron density. *Phys. Rev. B* 37, 785–789.

Michalski, M.C., Januel, C. (2006). Does homogenization affect the human health properties of cow's milk?. *Trends Food Sci. Technol.* 17, 423–437.

Reed, A.E., Curtiss, L.A., Weinhold F. (1988). Intermolecular interactions from a natural bond orbital, donor-acceptor viewpoint. *Chem. Rev.* 88, 899–926.

Reva, I.D., Plokhotnichenko, A.M., Stepanian, S.G., Ivanov, A.Y., Radchenko, E.D., Sheina, G.G., Blagoi, Y.P. (1995). The rotamerization of conformers of glycine isolated in inert gas matrices. An infrared spectroscopic study. *Chem. Phys. Lett.* 232, 141–148.

Selvarengan, P., Kolandaivel, P. (2004). Potential energy surface study on glycine, alanine and their zwitterionic forms. *J. Mol. Struct. Theochem.* 671, 77–86.

Stepanian, S.G., Reva, I.D., Radchenko, E.D., Rosado, M.T.S., Duarte, M.L.T.S., Fausto, R., Adamowicz, L. (1998). Matrix-Isolation Infrared and Theoretical Studies of the Glycine Conformers. *J. Phys. Chem. A* 102, 1041–1054.

Wagner, I., Musso, H. (1983). New Naturally Occurring Amino Acids. *Angew. Chem. Int. Ed. Engl.* 22 (11), 816–828.

Weinhold, F., Landis, C.R. (2005). *Valency and Bonding. A Natural Bond Orbital Donor-Acceptor Perspective.* Cambridge University Press: New York.

## Theoretical and Experimental Vibrational Spectrum Analysis of Ionic Liquid 1-Ethyl-3-Methylimidazolium Chloride

Nihal KUŞ and Saliha ILICAN

Department of Physics, Science Faculty, Eskisehir Technical University, Yunus Emre  
Campus, 26470 Eskisehir, Turkey

### Abstract

In the present experimental study, 1-ethyl-3-methylimidazolium chloride (EMIM-Cl) in anion-cation form was studied both dispersed in KBr matrix and as a thin film. The studied environments of ionic liquids were the liquid and crystalline phases, and they were similar. In both environments, the dominant forces are of Coulomb type, between the ions. Theoretical studies were undertaken at the DFT(B3LYP)/6-311++G(2d,2p) level of approximation using the GAUSSIAN 09 suit of programs. EMIM cation has two conformers with minimum energy obtained by scanning the C-N-C-C dihedral angle.

**Keywords:** Ionic liquid, 1-ethyl-3-methylimidazolium chloride, DFT, IR.

### 1. INTRODUCTION

Ionic liquids (ILs) are known as salts and exist in liquid form at and below 100 °C. Therefore, they are also called molten salts. There have been a lot of research and reports about ILs [1]. In recent years, a series of imidazolium anti-microbial activity and biodegradability related to ILs have been published. Heterocyclic systems with imidazolium or pyridinium polar head groups, which are found in some of the more widely used ionic liquids, have definite advantages such as excellent transfection profiles and low cytotoxicity [2].

In present study, the structural and vibrational frequencies of 1-ethyl-3-methylimidazolium (EMIM) cation form and its Cl anion form (EMIM-Cl) were investigated experimentally and theoretically.

### 2. METHODS

1-Ethyl-3-methylimidazolium chloride (EMIM-Cl) was commercial products supplied by Aldrich and at room temperature, it is solid (m.p. 75 °C). Infrared spectra (IR) of the compound were obtained in a BOMEM MB104 FTIR spectrometer with ZnSe optics with 4 cm<sup>-1</sup> spectral resolution. EMIM-Cl was studied both dispersed in KBr matrix and as a thin film. Temperature variation studies were undertaken using a SPECAC infrared variable temperature cell connected to a temperature digital controller (Red Lions). The estimated uncertainty in temperature is ±2 °C.

Theoretical studies were undertaken at the DFT(B3LYP)/6-311++G(2d,2p) level of approximation via the GAUSSIAN 09 suit of programs. Normal coordinate analyses were performed with the BALGA program.

### 3. RESULTS AND DISCUSSION

Figs. 1 and 2 show calculated molecule structure of EMIM cation conformers and with Cl anion pairs, respectively, using DFT/B3LYP/6-311++g(2d,2p) method. EMIM-1 and EMIM-2 are C<sub>1</sub> (double degenerated by-symmetry form) and C<sub>s</sub> symmetry form while in our previous study stable DMIM conformation is C<sub>2v</sub>. In agreement with previously reported ab initio and DFT(B3LYP)/6-31G\* calculations [3, 4], the present higher level calculations predict a single stable conformation for EMIM, where the methyl and ethyl groups are oriented in such a way that one of their C-H bonds is syn-periplanar to the N1-H bond, and two stable conformations for EMIM, with the C<sub>1</sub> symmetry one being more stable than the C<sub>s</sub> symmetry form about 2.4 kJ mol<sup>-1</sup> while calculated by DFT/B3LYP/6-311++g(2d,2p) method [5, 6].

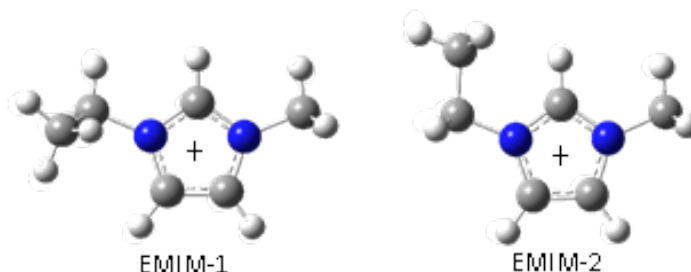


**Figure 1.** Calculated for two different minimum conformations of EMIM.

EMIM-1 was the most stable conformers. In this study, the most stable form of EMIM-1 cation and chlorine anion forms were taken into consideration. Three different energy states of chlorine were calculated (DFT/B3LYP/6-311++g(2d,2p)) (Fig. 2).

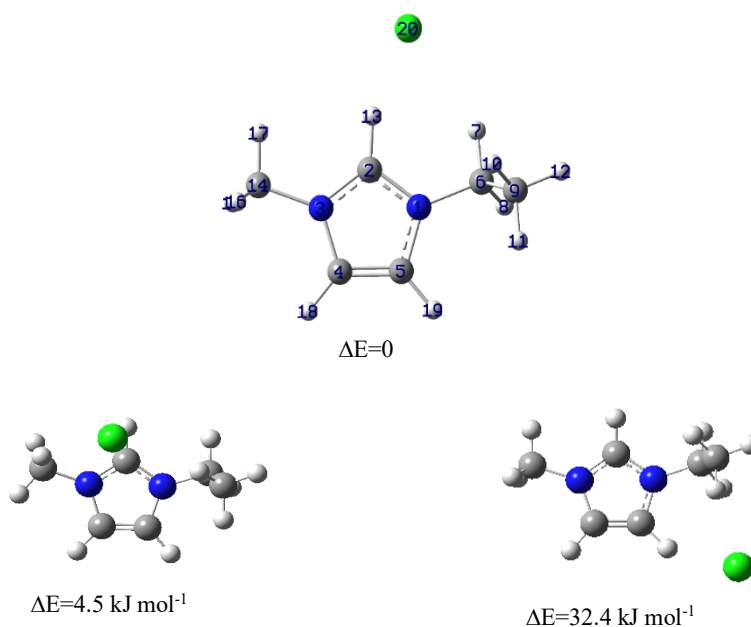


**Figure 2.** Scheme of EMIM-Cl most stable conformer with adopted atom number and its other forms.

The calculated spectra fit very nicely the experimental data (though overestimating the effect on both frequency and intensity of the H-bond between C2H and the cation in the case of EMIM-Cl). The spectra of the compounds practically do not change with temperature; in particular, the spectra

of the liquid and crystalline phases are identical, indicating the molecular environment is very similar in these two phases. The spectra of EMIM-Cl are essentially the sum-spectra of their constituting ions. This result supports the idea that in both the crystalline and liquid phases the dominant intermolecular forces are of electrostatic nature, between the ions. However, the observed changes upon temperature variation and differences between the features in the experimental spectra related with the imidazolium moiety and those calculated for the cations are particularly noticed for the bands associated with the C2-H bond, which is the one known to interact strongly with the anion through a hydrogen-bond. This observation stresses the non-neglectable importance of the C2-H...(anion) H-bond like interaction in the studied compounds.

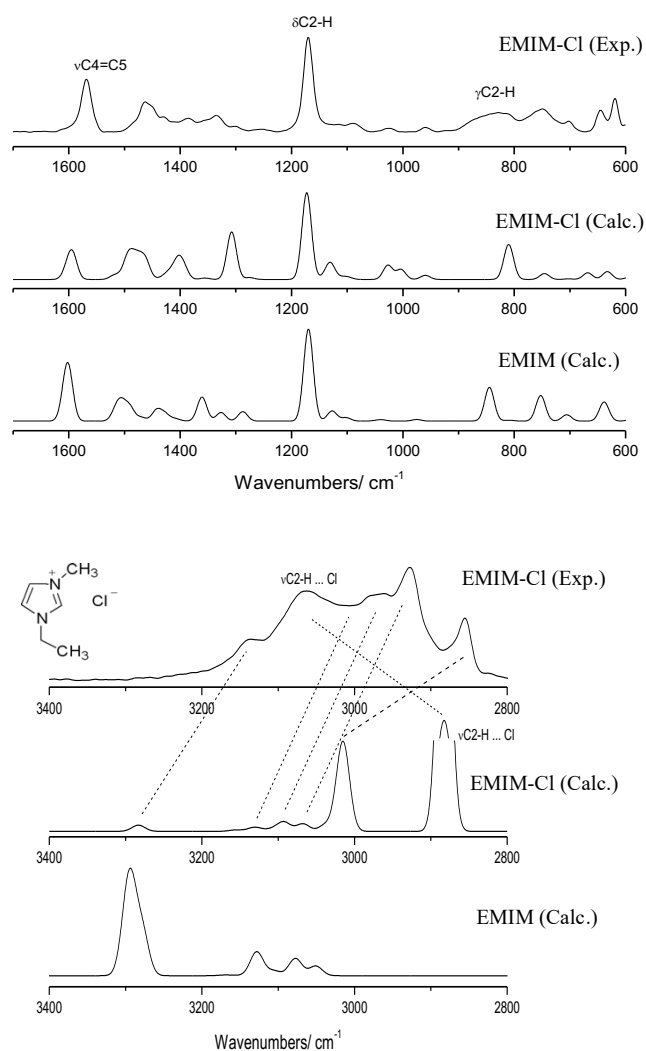


**Figure 3.** Experimental IR spectra for thin films of EMIM-Cl and calculated spectra for EMIM and EMIM-Cl. ((a) 3400-2800  $\text{cm}^{-1}$  region; (b) 1700-600  $\text{cm}^{-1}$  region).

From the ring bond lengths, it is possible to calculate the level of p-electron delocalization through the aromaticity index Harmonic Oscillator Measure of Aromaticity (HOMA), described by

Kruszewski and Krygowski [7-9], where  $n$  is the number of bonds considered belong to C-C and C-N bonds, and  $\alpha$  is the empirical constant, which are 257.7 and 93.52, respectively. If HOMA is equal to zero, a non-aromatic system; however, a fully aromatic system occurs when HOMA is equal to one. In this equation  $R_i$  gives the length of the running bond (Table 2). The reference values  $R_{opt}$  for the C-C bond is 1.3963 Å, whereas for the C-N bond it is taken as 1.3288 Å [10, 11]. The calculated HOMA index for DMIM about 0.5. It cannot be mentioned as a full aromaticity for this value, even the aromaticity is low degree. In a previous study, similar results were reported for the  $\alpha$ -pyrone ring in coumarin [11].

**Table 1.** Results of the normal coordinate analyses for EMIM-1

| Approximate <sup>b</sup><br>Description | Symmetry | Calculated<br>Frequency | Intensity | PED <sup>c</sup>   |
|---|----------|-------------------------|-----------|--|
| $\nu(\text{C2-H})$                      | A'       | 3300                    | 9.0       | $\nu(\text{C2-H})(83.8)$   |
| $\nu(\text{C5-H})$                      | A'       | 3294                    | 31.7      | $\nu(\text{C5-H})(44.5) + \nu(\text{C4-H})(39.0) + \nu(\text{C2-H})(15.3)$   |
| $\nu(\text{C4-H})$                      | A'       | 3278                    | 16.4      | $\nu(\text{C4-H})(52.6) + \nu(\text{C5-H})(46.9)$  |
| $\nu(\text{CH3})_{as''}$                | A'       | 3170                    | 0.3       | $\nu(\text{CH3})_{as''}(74.4) + \nu(\text{CH3})_{as'}(24.8)$   |
| $\nu(\text{CH3})_{as'}$                 | A'       | 3155                    | 0.1       | $\nu(\text{CH3})_{as'}(75.1) + \nu(\text{CH3})_{as''}(25.0)$   |
| $\nu(\text{CH3})_{as'(et)}$             | A'       | 3129                    | 2.6       | $\nu(\text{CH3})_{as'(et)}(95.9)$  |
| $\nu(\text{CH3})_{as''(et)}$            | A'       | 3128                    | 6.6       | $\nu(\text{CH2})_{as}(55.6) + \nu(\text{CH3})_{as''(et)}(44.6)$  |
| $\nu(\text{CH2})_{as}$                  | A'       | 3106                    | 1.9       | $\nu(\text{CH3})_{as''(et)}(55.6) + \nu(\text{CH2})_{as}(44.7)$  |
| $\nu(\text{CH3})_s$                     | A'       | 3078                    | 3.3       | $\nu(\text{CH3})_s(98.5)$  |
| $\nu(\text{CH2})_s$                     | A'       | 3077                    | 3.4       | $\nu(\text{CH2})_s(97.4)$  |
| $\nu(\text{CH3})_{s(et)}$               | A'       | 3051                    | 3.7       | $\nu(\text{CH3})_{s(et)}(94.9)$  |
| $\nu(\text{C4=C5})$                     | A'       | 1607                    | 15.1      | $\nu(\text{C4=C5})(38.3) + \nu(\text{N3=C2})(16.3) + \delta(\text{C5-H})(12.7)$  |
| $\delta(\text{C2-H})$                   | A''      | 1601                    | 53.0      | $\nu(\text{C4=C5})(30.4) + \delta(\text{C2-H})(16.4) + \nu(\text{N1-C2})(14.0)$  |
| $\delta(\text{CH3})_{as'}$              | A''      | 1515                    | 7.9       | $\delta(\text{CH3})_{as'}(66.9)$   |
| $\delta(\text{CH3})_{as''(et)}$         | A''      | 1515                    | 3.2       | $sc(\text{CH2})(33.5) + \delta(\text{CH3})_{as''(et)}(30.1) + \delta(\text{CH3})_{as'}(10.8) + \delta(\text{CH3})_{as'-A}(10.0)$     |
| $sc(\text{CH2})$                        | A''      | 1507                    | 5.1       | $sc(\text{CH2})(47.8) + \delta(\text{CH3})_{as''-A}(31.4) + \delta(\text{CH3})_{as'-A}(10.3)$  |
| $\delta(\text{CH3})_{as'(et)}$          | A''      | 1505                    | 12.0      | $\delta(\text{CH3})_{as'(et)}(69.1) + \delta(\text{CH3})_{as''(et)}(21.4)$   |
| $\delta(\text{CH3})_{as''}$             | A''      | 1491                    | 14.8      | $\delta(\text{CH3})_{as''}(88.7)$  |
| $\delta(\text{CH3})_s$                  | A''      | 1470                    | 4.0       | $\delta(\text{CH3})_s(86.6)$   |
| $w(\text{CH2})$                         | A''      | 1442                    | 12.0      | $\delta(\text{CH3})_{s(et)}(31.7) + w(\text{CH2})(20.8)$   |
| $\delta(\text{CH3})_{s(et)}$            | A''      | 1427                    | 7.6       | $\delta(\text{CH3})_{s(et)}(64.4) + w(\text{CH2})(12.9)$   |
| $\nu(\text{N3-C4})$                     | A'       | 1409                    | 2.5       | $\nu(\text{N3-C2})(24.8) + \nu(\text{N3-C4})(21.2) + \delta(\text{CH3})_{as'}(12.2)$   |
| $\nu(\text{N1-C2})$                     | A'       | 1361                    | 26.6      | $w(\text{CH2})(27.5) + \nu(\text{N1-C2})(17.8) + \nu(\text{N1-C6})(10.0)$  |
| $\nu(\text{N1-C5})$                     | A'       | 1327                    | 7.9       | $\nu(\text{N1-C5})(15.9) + \nu(\text{N3-C14})(14.2) + \nu(\text{N3-C4})(14.1) + \delta(\text{C5-H})(9.8)$                            |
| $t(\text{CH2})$                         | A''      | 1326                    | 1.5       | $t(\text{CH2})(87.4) + \gamma(\text{CH3})''_{(et)}(11.2)$  |
| $\delta(\text{C4-H})$                   | A''      | 1288                    | 10.4      | $\delta(\text{C2-H})(30.9) + \delta(\text{C4-H})(16.0) + \delta(\text{C5-H})(14.8)$  |
| $\delta(\text{C2-H})$                   | A''      | 1170                    | 100.6     | $\delta(\text{C2-H})(28.4) + \nu(\text{N1-C6})(16.2) + \nu(\text{N3-C14})(12.7) + \nu(\text{N1-C5})(9.8) + \delta(\text{C4-H})(9.7)$ |
| $r(\text{CH2})$                         | A''      | 1167                    | 1.3       | $r(\text{CH2})(43.8) + \gamma(\text{CH3})''_{(et)}(39.0)$  |
| $\gamma(\text{CH3})'$                   | A''      | 1154                    | 0.2       | $\gamma(\text{CH3})'(61.2) + \gamma(\text{CH3})''(19.8) + \delta(\text{CH3})_{as''}(9.7)$  |
| $\delta(\text{C5-H})$                   | A''      | 1127                    | 11.2      | $\delta(\text{C5-H})(34.8) + \delta(\text{C4-H})(25.9) + \nu(\text{C4=C5})(19.2) + \nu(\text{N1-C5})(9.6)$                           |
| $\gamma(\text{CH3})'_{(et)}$            | A''      | 1107                    | 0.3       | $\gamma(\text{CH3})'_{(et)}(34.7) + \nu(\text{C6-C9})(13.3) + sc(\text{N1-C9})(9.7)$   |
| $\gamma(\text{CH3})''$                  | A''      | 1102                    | 3.5       | $\gamma(\text{CH3})''(33.1) + \gamma(\text{CH3})'(11.0) + \gamma(\text{CH3})'_{(et)}(10.5)$  |
| $\delta$ ring                           | A''      | 1049                    | 0.4       | $\nu(\text{N1-C5})(27.3) + \delta$ ring (19.4) + $\nu(\text{C6-C9})(18.8)$   |
| $\delta$ ring'                          | A''      | 1038                    | 1.4       | $\delta$ ring' (46.2) + $\nu(\text{N3-C4})(17.0)$  |
| $\nu(\text{C6-C9})$                     | A'       | 975                     | 1.7       | $\nu(\text{C6-C9})(39.2) + \gamma(\text{CH3})'_A(26.1) + \delta$ ring (18.3)   |
| $\gamma(\text{C5-H})$                   | A''      | 879                     | 0.1       | $\gamma(\text{C5-H})(57.3) + \gamma(\text{C4-H})(52.2)$  |
| $\gamma(\text{C2-H})$                   | A''      | 845                     | 37.3      | $\gamma(\text{C2-H})(72.5) + \gamma(\text{C4-H})(9.9)$   |
| $\gamma(\text{CH3})''_{(et)}$           | A''      | 809                     | 0.9       | $r(\text{CH2})(43.3) + \gamma(\text{CH3})''_{(et)}(32.6) + \gamma(\text{C2-H})(12.1)$  |
| $\gamma(\text{C4-H})$                   | A''      | 753                     | 28.4      | $\gamma(\text{C4-H})(43.0) + \gamma(\text{C5-H})(41.1) + \gamma(\text{C2-H})(15.4)$  |
| $\nu(\text{N3-C14})$                    | A'       | 706                     | 7.0       | $\delta$ ring' (30.6) + $\nu(\text{N3-C14})(28.2) + \nu(\text{N1-C6})(17.0)$   |

|                   |     |     |      |  |
|-------------------|-----|-----|------|--|
| $\tau$ ring'      | A'' | 639 | 18.7 | $\tau$ ring' (95.9)  |
| $\tau$ ring       | A'' | 635 | 2.7  | $\tau$ ring (100.4)  |
| $\nu$ (N1-C6)     | A'  | 591 | 1.3  | $\nu$ (N1-C6)(22.8) + $\delta$ ring (21.3) + $\nu$ (N3-C14)(20.8)  |
| sc(N1-C9)         | A'' | 447 | 0.8  | $\delta$ (N1-C6)(29.5) + $\delta$ (N3-C14)(17.3) + sc(N1-C9)(15.1) + $\nu$ (N1-C6)(10.8) + $\nu$ (C6-C9)(10.7) |
| $\delta$ (N3-C14) | A'' | 355 | 0.5  | $\delta$ (N3-C14)(56.3) + sc(N1-C9)(26.7)  |
| $\tau$ (C6-C9)    | A'' | 299 | 0.2  | $\tau$ (C6-C9)(80.2) + $\gamma$ (N1-C6)(18.4)  |
| $\gamma$ (N3-C14) | A'' | 247 | 0.7  | $\gamma$ (N3-C14)(62.8) + $\gamma$ (N1-C6)(18.2) + $\tau$ (C6-C9)(14.3)  |
| $\delta$ (N1-C6)  | A'' | 187 | 0.6  | $\delta$ (N1-C6)(53.4) + sc(N1-C9)(25.8) + $\delta$ (N3-C14)(14.3)   |
| $\gamma$ (N1-C6)  | A'' | 168 | 3.5  | $\gamma$ (N1-C6)(60.9) + $\gamma$ (N3-C14)(23.5)   |
| $\tau$ (N1-C6)    | A'' | 72  | 0.1  | $\tau$ (N1-C6)(97.0)   |
| $\tau$ (N3-C14)   | A'' | 31  | 0.3  | $\tau$ (N3-C14)(104.6)   |

<sup>a</sup> Frequencies:  $\text{cm}^{-1}$ ; intensities:  $\text{km mol}^{-1}$ .  $\nu$ : stretching,  $\delta$ : bending,  $\gamma$ : rocking,  $\tau$ : torsion. <sup>b</sup> The description is given in the PED form (last column of the Table). <sup>c</sup> PED's higher than 10 % are included.

**Table 2.** Calculated bond lengths for EMIM-1

|                                 | Bond lengths/ Å | X-ray [6] |
|---------------------------------|-----------------|-----------|
| N1-C2                           | 1.334           | 1.327     |
| N1-C5                           | 1.380           | 1.376     |
| N3-C2                           | 1.336           |           |
| N3-C4                           | 1.380           | 1.367     |
| C4-C5                           | 1.358           | 1.352     |
| N3-C <sub>m</sub>               | 1.469           | 1.449     |
| N1-C <sub>et</sub>              | 1.486           | 1.489     |
| C <sub>et</sub> -C <sub>m</sub> | 1.518           | 1.472     |
| C2-H                            | 1.074           |           |
| C4-H                            | 1.074           |           |
| C5-H                            | 1.074           |           |

#### 4. CONCLUSIONS

The EMIM-Cl anion and cation forces was the Coulomb type interaction and ionic liquid was found to exhibit local environments in liquid phases. In this study, the temperature was increased up to 150 oC from room temperature. Since the spectra of 125 oC were observed better than the others, this spectrum was plotted. The obtained EMIM-Cl IR spectra of the liquid and crystalline phases was not belonging to temperature, because the spectrum taken at each temperature did not change. Nevertheless, some shifts of C2H vibration were observed. These shifts result from the interaction between the imidazolium ring and the anion. In order to determine normal coordinates and potential energy distributions for EMIM-Cl were used BALGA program.

#### ACKNOWLEDGEMENT

This work was supported by the Eskisehir Technical University Commission of Research Project under grant no: 19ADP130.

#### REFERENCES

- [1] K. R. Seddon, *Nat. Mater.*, 2003, 2, 363.
- [2] a) J. Pernak, K. Sobaszekiewicz and I. Mirska, *Green Chem.*, 2003, 5, 52; b) P. J. Scammells, J. L. Scott and R. D. Singer, *Aust. J. Chem.*, 2005, 58, 155; c). N. Gathergood and P. J. Scammells,

Aust. J. Chem., 2002, 55, 557. d) P. Wasserscheid "Volatile times for ionic liquids" Nature, 2006. Vol 439.

- [3] E. A. Turner, C. C. Pye and R. D. Singer, J. Phys. Chem. A, 2003, 107, 2277.
- [4] S. A. Katsyuba, E. E. Zvereva, A. Vidiš, P. J. Dyson, J. Phys. Chem. A, 2007, 111, 352.
- [5] H.-C. Chang, J.-C. Jiang, W.-C. Tsai, G.-C. Chen, S. H. Lin, J. Phys. Chem. B. 2006, 110, 3302.
- [6] A. Elaiwi, P. B. Hitchcock, K. R. Seddon, N. Srinivasan, Y.-M. Tan, T. Welton, J. A. Zora, J. Chem. Soc., Dalton Trans., 1995, 3467.
- [7] J. Kruszewski and T. M. Krygowski, Tet. Lett., 1972, 13, 3839.
- [8] T. M. Krygowski, J Chem Inform. Comp. Sci., 1993, 33, 70.
- [9] T. M. Krygowski and M. Cyranski, Tetrahedron, 1996, 52, 1713.
- [10] C. A. Morrison, B. A. Smart, D. W. H. Rankin, H. E. Robertson, M. Pfeffer, W. Bodenmuller, R. Ruber, B. Macht, A. Ruoff and V. Typke, J. Phys. Chem. A, 1997, 101, 10029.
- [11] N. Kuş, S. Breda, I. D. Reva, E. Tasal, C. Ogretir and R. Fausto, Photochem. Photobiol., 2007, 83, 1237.